NOAA Technical Report NOS CO-OPS 072
Ocean Systems Test and Evaluation Program

Test and Evaluation Report

For WaterLog® H-3612 Radar Sensor in CO-OPS Air Gap Applications

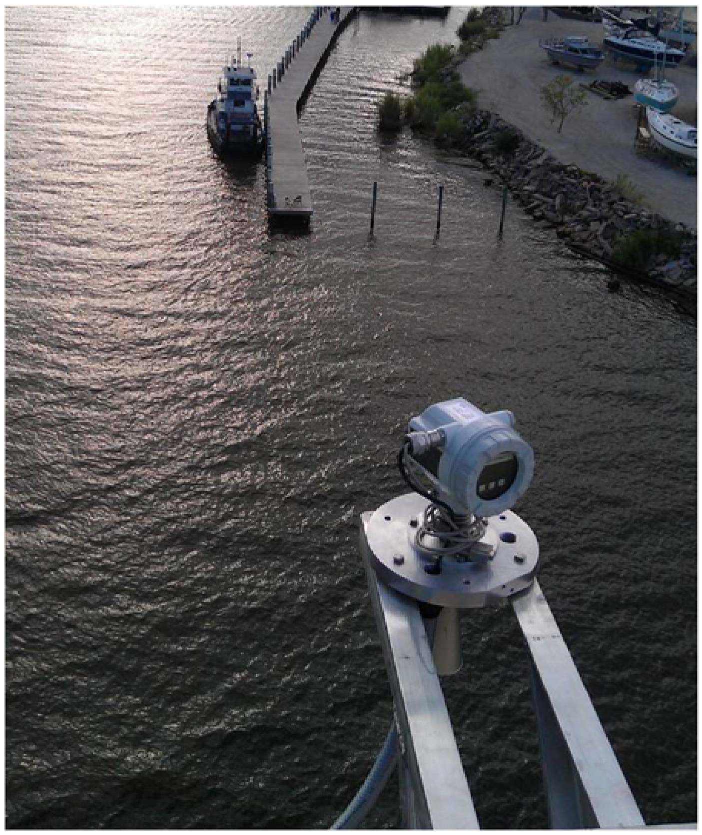

Silver Spring, Maryland
January 2013

noaa National Oceanic and Atmospheric Administration

U.S.DEPARTMENT OF COMMERCE
National Ocean Service
Center for Operational Oceanographic Products and Services

Department of Commerce
National Oceanic and Atmospheric Administration
National Ocean Service
Center for Operational Oceanographic Products and Services

The National Ocean Service (NOS) Center for Operational Oceanographic Products and Services (CO-OPS) provides the National infrastructure, science, and technical expertise to collect and distribute observations and predictions of water levels and currents to ensure safe, efficient and environmentally sound maritime commerce. The Center provides the set of water level and tidal current products required to support NOS' Strategic Plan mission requirements and to assist in providing operational oceanographic data/products required by NOAA's other Strategic Plan themes. For example, CO-OPS provides data and products required by the National Weather Service to meet its flood and tsunami warning responsibilities. The Center manages the National Water Level Observation Network (NWLON), a national network of Physical Oceanographic Real-Time Systems (PORTS®) in major U.S. harbors, and the National Current Observation Program, consisting of current surveys in near shore and coastal areas utilizing bottom mounted platforms, subsurface buoys, horizontal sensors and quick response real-time buoys. The Center: establishes standards for the collection and processing of water level and current data; collects and documents user requirements which serve as the foundation for all resulting program activities; designs new and/or improved oceanographic observing systems; designs software to improve CO-OPS' data processing capabilities; maintains and operates oceanographic observing systems; performs operational data analysis/quality control; and produces/disseminates oceanographic products.

Ocean Systems Test and Evaluation Program

The CO-OPS Ocean Systems Test and Evaluation Program (OSTEP) facilitates the transition of new technology to an operational status, selecting newly developed sensors or systems from the research and development community and bringing them to a monitoring setting. OSTEP provides quantifiable and defensible justifications for the use of existing sensors and methods for selecting new systems. The program establishes and maintains field reference facilities where, in cooperation with other agencies facing similar challenges, devices are examined in a non-operational field setting. Through OSTEP, sensors are evaluated, quality control procedures developed, and maintenance routines generated. The quality of the reference systems used in the field is assured by both rigorous traceable calibrations and redundant sensors.

NOAA Technical Report NOS CO-OPS072
Ocean Systems Test and Evaluation Program

Test and Evaluation Report

For WaterLog® H-3612 Radar Sensor in CO-OPS Air Gap Applications

Robert Heitsenrether
Winston Hensley

January 2013

U.S.DEPARTMENT OF COMMERCE
Penny Pritzker, Secretary

National Oceanic and Atmospheric Administration
Dr. Kathryn Sullivan

National Ocean Service
Dr. Holly Bamford, Assistant Administrator

Center for Operational Oceanographic Products and Services
Richard Edwing, Director

NOTICE

Ocean Systems Test and Evaluation Program

Test and Evaluation Report for the WaterLog® H-3612 Radar Sensor in CO-OPS Air Gap Applications

CO-OPS STATEMENT OF ACCEPTANCE

CO-OPS management personnel have reviewed this document and concur that the evaluated sensor/system, when deployed and implemented as described herein, meets the defined requirements and is suitable for operational use. While additional testing may lead to superior performance or more economical operation, the existing sensor/system configuration is sufficient as described.

01/18/13		18JAN13	
OSTEP Program Manager	Date	System Support and Evaluation Branch	Date
1/23/13		1/22/13	
Chief, Engineering Division	Date	Chief, Field Operations Division	Date
1/25/13		1/29/13	
Chief, Oceanography Division	Date	Chief, Information Systems Division	Date

1/29/13

Chief Scientist, CO-OPS — Date

1/28/13

Director, CO-OPS — Date

Table of Contents

List of Figures

List of Tables

Acknowledgements

The authors thank the following CO-OPS personnel for their contributions to this test and evaluation effort and resulting report:

Albert Sanford for his design of the sensor mount;

Warren Krug for his work on system integration and laboratory testing;

Grace Gray and Warren Krug for assistance with the field installation of the test system at Reedy Point, DE;

Helen Worthington for her assistance in the technical editing and formatting of this report and Brenda Via for her assistance in report production and publication.

Executive Summary

In 2005, the National Oceanic and Atmospheric Administration (NOAA) National Ocean Service (NOS) Center for Operational Oceanographic Products and Services (CO-OPS) completed the development, testing, and transition to operations of an air gap-bridge clearance measurement system for use in the CO-OPS Physical Oceanographic Real-Time System (PORTS®). The purpose of this measurement system is to provide real-time observations of the vertical distance from a bridge's lowest steel to the mean water level surface below, commonly referred to as air gap. The observation provides vessel pilots with decision support information that can decrease the likelihood of vessel overhead allisions with bridges. This development and test effort was motivated and supported by several PORTS® customers who were concerned with growing bridge allision risks resulting from significant increase in vessel size and vessel traffic across several U.S. ports and harbors.

Developed and transitioned to operations in 2005 by CO-OPS Ocean System Test and Evaluation Program (OSTEP), the air gap system employs a microwave band radar range sensor to measure the distance from a point on a bridge to the water surface below. The radar sensor selected for that system is a Miros model SM-094. Initial development efforts and several related reports and presentations clearly conveyed that microwave radar technology is the best choice for the PORTS® air gap measurement applications.

OSTEP has continued test and development efforts with radar range sensors for other CO-OPS applications, partly because of the success of the PORTS® air gap system. From 2008-2011, OSTEP expended significant effort to test and evaluate four different brands of radar range sensors to assess their suitability for use as primary water level sensors throughout the CO-OPS National Water Level Observation Network (NWLON). Three years of additional field and lab testing has resulted in a significant increase in CO-OPS' knowledge of microwave radar sensor technology, both through analysis of test data and hands-on field experience with sensors. Additional information about other available commercial-off-the-shelf sensor brands and models was also obtained through the effort. This wealth of knowledge gained through additional radar sensor testing for NWLON applications has been leveraged to support a number of improvements to existing operational air gap measurement systems. Recent improvements include enhanced laboratory test procedures and analysis tools, Sutron Xpert data collection platform software upgrades, and new mounting hardware designs.

Most recently, the OSTEP team has identified the Design Analysis WaterLog® H-3612 microwave radar as a potential alternative PORTS® air gap sensor, based on test results for NWLON applications. This sensor, already used in some CO-OPS water level applications, offers many advantages over CO-OPS' current operational sensor, the Miros SM-094. Motivated by the potential to improve existing PORTS® air gap systems, OSTEP conducted a series of laboratory and field tests on the WaterLog® H-3612 designed to assess the suitability for use in PORTS® air gap applications. All laboratory tests conducted indicate that the WaterLog® H-3612 meets CO-OPS operational standards. Field testing included the installation of a test WaterLog® sensor alongside an operational Miros SM-094 sensor at the PORTS® station on the Reedy Point, DE Bridge for eight months. WaterLog® and Miros sensors showed good agreement during the field test for air gap data collected and transmitted every 6 minutes. The monthly root mean squared deviation was less than 4 cm, and the monthly mean differences were all less than 6.2 cm; both values are well below the real-time air gap measurement accuracy requirement of ±15 cm, which CO-OPS established with prospective users during initial air gap system development efforts [1]. Based on laboratory and field test results included in this report, OSTEP has recommended use of the WaterLog® H-3612 radar sensor at CO-OPS operational air gap stations where the sensor's maximum 70-m range is not expected to be exceeded.

1.0 Introduction/Background

The National Oceanic and Atmospheric Administration (NOAA) National Ocean Service (NOS) Center for Operational Oceanographic Products and Services (CO-OPS) currently maintains 21 operational Physical Oceanographic Real-Time Systems (PORTS®) that provide critical information to support safe and efficient navigation throughout U.S. coastal regions. Real-time bridge clearance observations provided by PORTS® air gap systems have proven to be a valuable decision support tool for vessel pilots. Having access to these data can decrease the likelihood of vessel overhead allision with bridges. Many PORTS® customers have conveyed the critical need for air gap observations and as a result, the total number of CO-OPS operational air gap systems has continued to grow.

The CO-OPS Ocean Systems Test and Evaluation Program (OSTEP) team completed the development, testing, and transition to operations of the PORTS® air gap measurement system in 2005. Reference [1] describes all efforts that led to the air gap measurement systems that are in operation throughout PORTS® today, including a detailed description of why microwave radar sensor technology was selected for the air gap application, a review of system requirements, rationale for the selection of the Miros SM-094 sensor, and a discussion about the system error budget. OSTEP's rigorous test and development efforts have ensured proper use of the Miros SM-094 sensor, which has clearly served CO-OPS well for several years. Success of the PORTS® air gap measurement system prompted OSTEP to test microwave radar sensors for other CO-OPS applications. These include but are not limited to real-time water level measurements through the PORTS® and National Water Level Observation Network (NWLON) long-term observatories.

From 2008-2011, OSTEP expended significant effort to test and evaluate four radar range sensors, each from a different manufacturer, to assess their suitability for use as primary water level sensors throughout PORTS® and NWLON. These efforts resulted in the selection of the Design Analysis H-3611 microwave radar sensor for use in a number of specific CO-OPS water level applications. After three additional years of extensive laboratory and field tests, OSTEP acquired abundant knowledge about microwave radar sensor technology from both analysis of test data and hands-on field experience with sensors and related systems, as well as more information about different commercial-off-the shelf microwave radar sensors.

The insight gained from the most recent microwave radar sensor testing for NWLON applications has been leveraged to support a number of improvements to existing operational air gap measurement systems. Some improvements incorporated into existing systems include upgraded software in air gap data collection platforms (DCPs), implementation of improved sensor pre-deployment test procedures and related data analysis tools, and modified mounting hardware. Most significant was a recommendation to test and evaluate the Design Analysis WaterLog® H-3612 as a prospective alternative for use in PORTS® air gap applications.

The WaterLog® H-3612 is a longer range version of the H-3611, which is the radar sensor that OSTEP selected for use in several operational NWLON and PORTS® water level observatories.

Except for a few minor hardware/software adjustments and a slightly lower resolution (±3 mm compared to the ±1 mm resolution of the H-3611) required for obtaining longer range measurements, the H-3612 is almost identical to the H-3611. OSTEP's initial recommendation to test and evaluate the H-3612 radar for air gap applications is based on the many advantages and benefits that this sensor offers over existing air gap sensors, including:

- Lower power requirements due to signal type; H-3612 uses a short pulse signal while Miros SM-094 transmits a continuous modulated frequency waveform.
- Simpler SDI 12 interface integration with Sutron Xpert DCP.
- Better sensor configuration interface via GUI-based software tools which include capability to clearly plot and record sample return signals after installation.
- More robust hardware; easier to mount, reference sensor zero, and survey to.
- Less expensive than Miros SM-094

Encouraged by these advantages, OSTEP conducted a series of laboratory, crane lift, and field tests on the WaterLog® H-3612. Initial laboratory testing included a series of five tests that have been recommended for all radar sensors to be used in operational water level applications [2]. All lab tests yielded good results. Next, an overwater crane lift test was conducted at a marine facility on the Elizabeth River in Norfolk, VA. The test involved using a crane to position a multi-sensor platform over a relatively calm water surface at a series of different heights. The platform included three Miros SM-094 sensors, a Laser Technology, Inc. (LTI) Universal Laser Sensor (ULS), and a test H-3612. Measurements from the test WaterLog® H-3612 showed excellent agreement with the three Miros SM-094 sensors. For a final field test, a WaterLog® H-3612 was installed alongside the operational Miros SM-094 sensor at the Reedy Point, DE, PORTS® air gap system. The two sensors' measurements showed agreement that is within the existing air gap system accuracy requirement of ±15 cm.

The following report contains a description of each set of tests conducted with the WaterLog® H-3612 along with a summary of results. As discussed in the final section, all test results have led to the recommendation to use the WaterLog® H-3612 radar sensor at CO-OPS operational air gap stations where the sensor's maximum 70-m range is not expected to be exceeded.

2.0 Test Results

This section describes the details of three different sets of tests that OSTEP conducted with the WaterLog® H-3612 radar sensor: 1) laboratory verification, 2) over-water crane lift, and 3) field testing at a CO-OPS operational air gap system site. A summary of data collected and results from each test is included.

2.1 Laboratory Testing

Initial laboratory testing of the WaterLog® H-3612 sensor included the series of five tests described in [2]. The five-test procedure was developed based on extensive evaluation of the microwave radar sensor for water level applications and is designed to significantly decrease the likelihood of sensor problems occurring in the field. The five laboratory tests, listed in the order that they were conducted on the test WaterLog® H-3612, are:

1. Fixed Target Test for Resolution Verification
2. Sensor Offset Derivation
3. Time Response Verification
4. Range Accuracy Verification
5. Dynamic Liquid Target Test

OSTEP has recommended the requirement to conduct this five-test procedure and document the results for every radar range sensor prior to field deployment. The following paragraphs provide a description of each laboratory test.

2.1.1 Fixed Target Test for Resolution Verification

The first laboratory test involved setting up the H-3612 sensor in a secure mount to aim horizontally at a flat, fixed target and allowing the sensor to record 1-Hz range measurements for two hours. The main objective of this test was to obtain a time series from which an observed sensor resolution can be obtained, and any sensor noise (beyond digitization) can be detected and quantified.

The H-3612 sensor was securely mounted to aim directly at a flat, fixed sheet of aluminum placed a little more than 3 m away from the sensor. Internal settings for this test were configured for measuring range to a solid target. The sensor and target were oriented so that the resulting sensor signal path was as close to 90 degrees as possible to the aluminum sheet surface.

The manufacturer's specified resolution for the H-3612 is ±3 mm, which is slightly larger than the specified ±1 mm resolution of the shorter range H-3611. Figure 1 shows a plot of 1-Hz range series collected during the fixed target test with the WaterLog® H-3612, serial number (SN) 1026 (top panel). Also included is an example of the same type of test data collected from a short-range (40 m) H-3611 during a fixed target test. Figure 2 shows the frequency spectra calculated from both sensors' time series in fig. 1. Comparison of the two sensors' time series and frequency spectra indicates the slightly lower resolution of the H-3612 as compared to the H-3611, which is expected. Figure 3 shows a distribution of first differences calculated between subsequent 1-Hz points in the H-3612 range series in fig. 1. The largest difference between subsequent 1-Hz points is 3 mm. All results from the fixed target test shown in figs. 1-3 indicate that the H-3612 sensor is within the ±3 mm resolution specification.

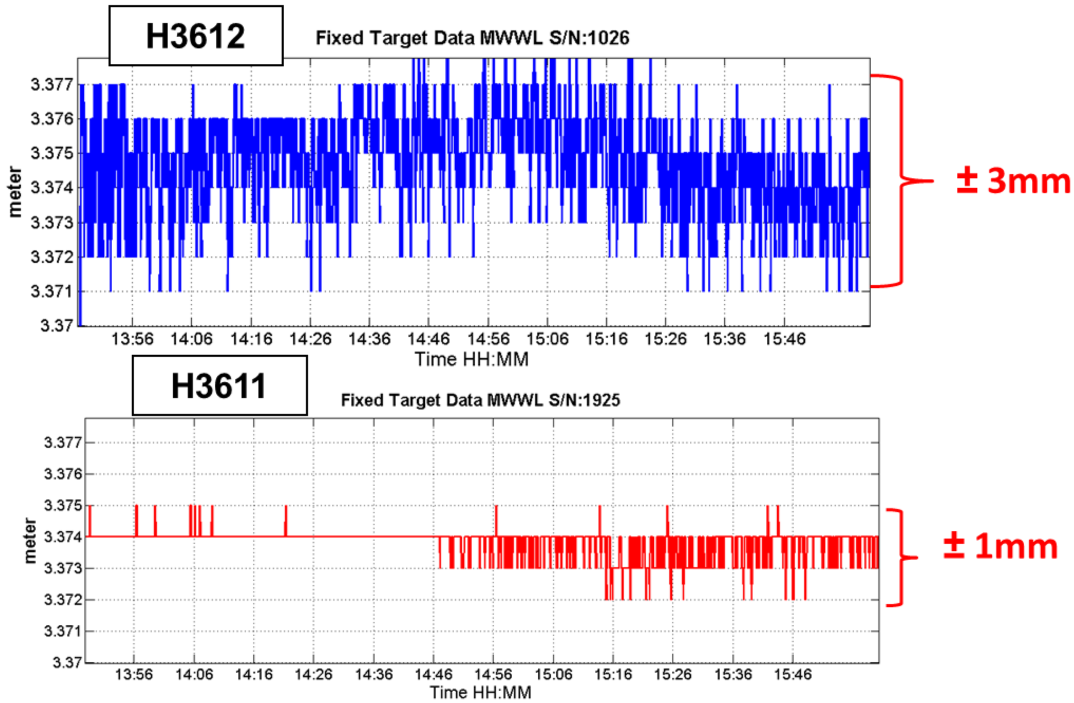

Figure 1. 1-Hz range time series collected during a fixed target lab test with a long range H-3612 (top) and a short range H-3611 (bottom).

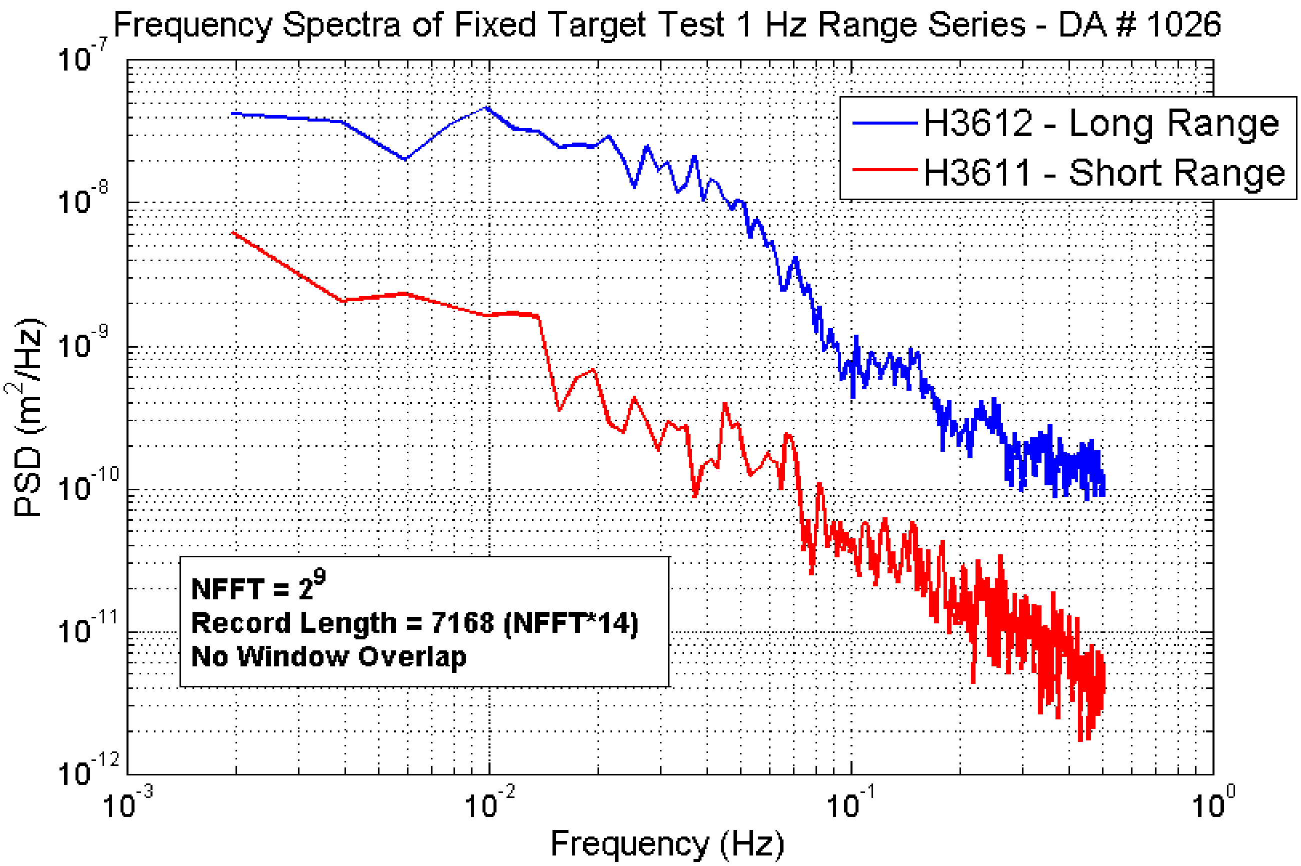

Figure 2. Frequency spectra calculated from the 1-Hz range time series shown in fig. 1.

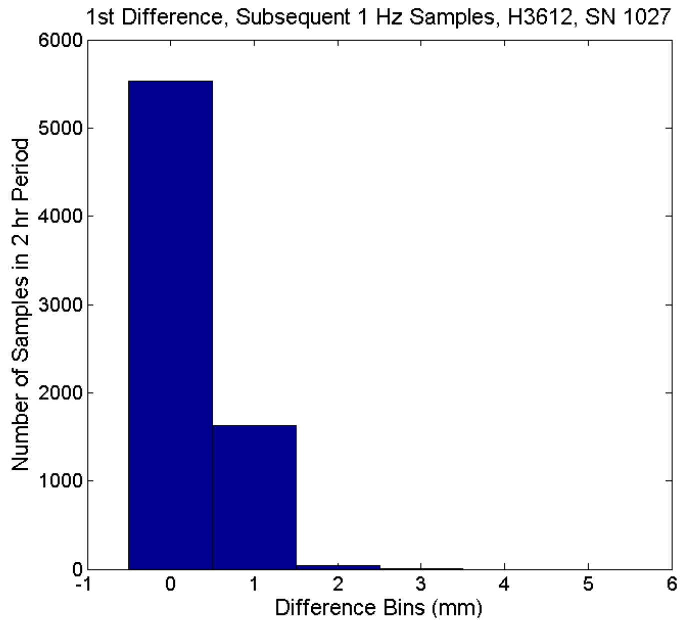

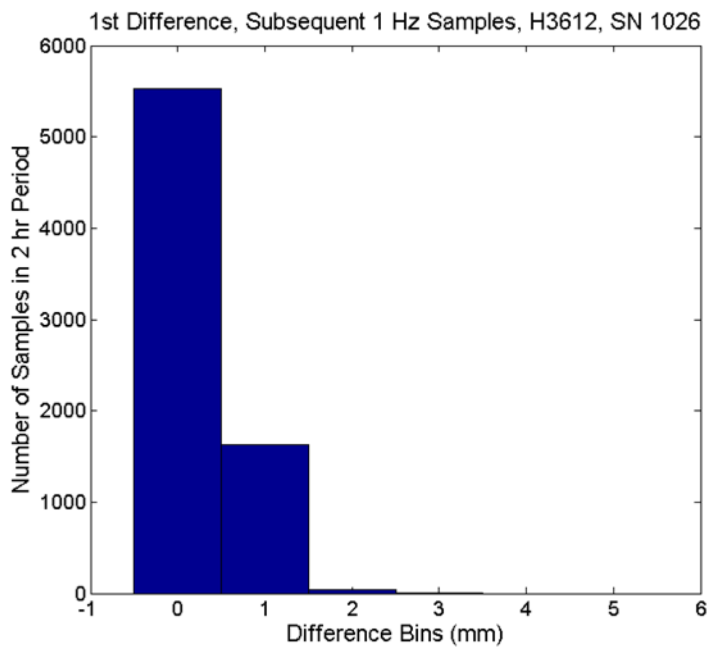

Figure 3. Histogram of first differences between subsequent 1-Hz range values shown in fig. 1, measured by H-3612.

2.1.2 Sensor Offset Derivation

Once the H-3612 test sensor was confirmed to be performing within resolution specifications, measurements were collected to calculate a sensor offset (SO), the distance from the bottom of the sensor's mounting plate to the zero range point (section 2.3.3 provides further discussion on SO). Laboratory measurements collected to date with the H-3611 indicate that the differences between the zero point and the bottom of the mounting flange can vary among the sensors within

±1.5 cm. The previously developed method for measuring an SO was employed for both of OSTEP's test H-3612 sensors using the special mount shown in fig. 4. Table 1 contains the resulting SO values. For more detail on the procedure, see [3] and for information on how SO is applied to water level derivations, see [2].

Figure 4. Sensor offset measurement mount designed at the Chesapeake Instrument Laboratory (CIL) by A. Sanford.

Table 1. Sensor offsets for two OSTEP H-3612 test units**.**

Sensor Serial #	Sensor Offset (m)
1026	0.016
1027	0.007

2.1.3 Time Response Verification

A time response test was conducted to verify that the sensor responds to a moving target as expected when configured in the **Fast Mode**. When in **Fast Mode**, the sensor tracks target motions with a time response of approximately 5 s. The setup is similar to that of the fixed target test, with the radar mounted to aim horizontally at a flat, metal target, except the target will undergo back and forth range motions relative to the sensor. An LTI ULS is included in the sensor mount. Although a ULS's absolute range measurement accuracy is known to be less than that of a WaterLog® radar sensor, the ULS can respond to range changes much faster than 1 s, providing an excellent reference for the true start and stop times of target motion.

Comparison of radar range measurements are used to confirm that the sensor can track short, gradual range changes and to quantify the sensor's response time. Automated target motion was accomplished by using a small section of framed aluminum screen mounted atop a small automated carriage on wheels. Figure 5 shows one such setup that can be used to collect radar time response test data. Ranges measured by the H-3612 radar sensor during the time response test shown in fig. 6 yield the expected result.

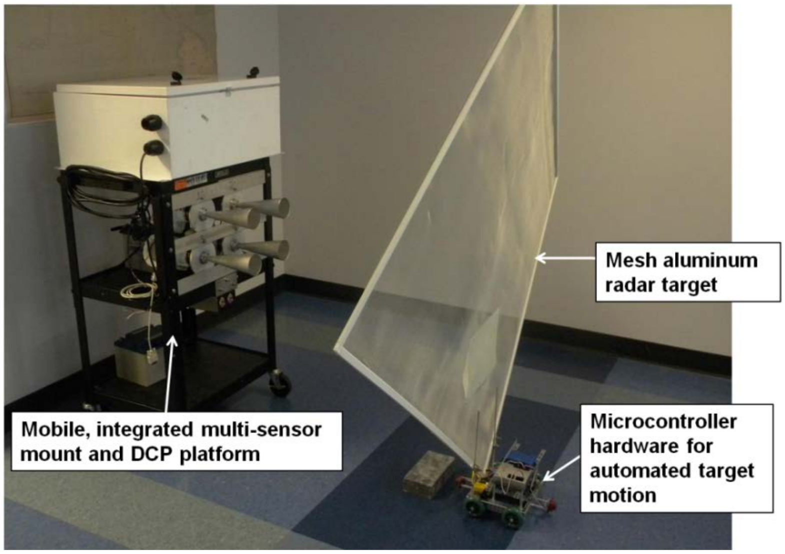

Figure 5. Example of radar time response test setup.

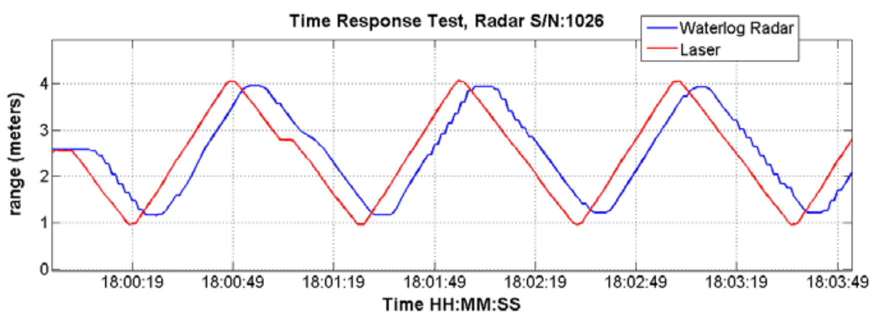

Figure 6. 1-Hz ranges measured by test WaterLog® H-3612 radar and reference ULS during the time response test.

2.1.4 Range Accuracy Verification

A range accuracy verification test was conducted with the H-3612, which involved collecting range measurements to a fixed target over a series of discrete sensor-to-target ranges. Once again, the sensor was fixed in a mount aimed toward a flat, fixed target with sensor transmission path aligned as close to the normal 90-degree angle as possible to the target face. The air gap target range rail system, located in the back ware yard of the CO-OPS Chesapeake, VA facility, was used for this test (currently under construction, fig. 7). Both of OSTEP's test H-3612 radar sensors were placed in a mount at one end of the range, along with two other H-3611 sensors (which were being tested for other purposes at the same time). The resulting sensor height above ground was approximately 2 m. The target used during this test was a sheet of aluminum on a stand that was designed to sit atop the set of I-beam railings (fig. 8).

Figure 7. The air gap target range rail system at the CO-OPS Chesapeake ware yard.

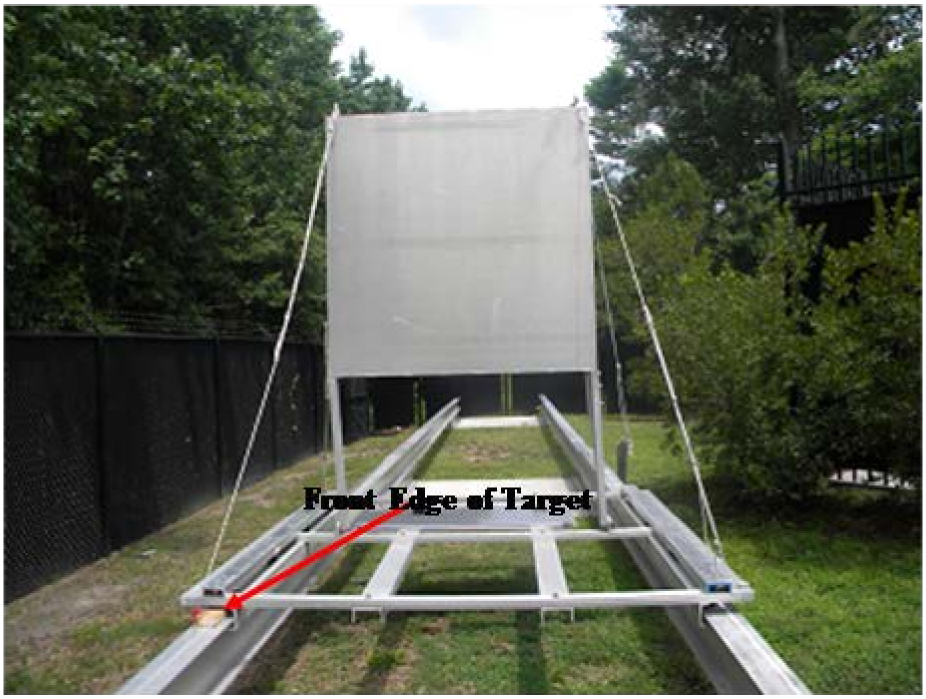

Figure 8. Metal target used during range verification laboratory test.

Obtaining measurements that will be useful for verification of the radar sensor's range accuracy remains a challenge given the current design of the CO-OPS Chesapeake's target range rail system; however, a best attempt was made with the available setup and equipment. The procedure involved collecting measurements across five discrete sensor-to-target ranges of 2 m, 4 m, 6 m, 8 m, and 12 m. Data collected for ranges beyond 12 m with a sensor aimed horizontally on the target rail system will be suspect due to the radar sensor's 8° dispersive beam (the radar's sensing footprint width increases linearly with range [4]). The impact of radar signal interaction with the ground and scenarios where target area is a small percentage of the radar footprint width are not fully understood at this point.

A NIST-traceable steel tape was used to obtain a reference measurement of target range for comparison with radar measurements. Measuring a reference range value directly from a radar sensor's flange to the target face using a tape is not practical on the rail system, so an alternative approach was taken. At the start of the test, radar range measurements were collected for 1 min with the target placed at the beginning of the rail system, a little less than 1 m from the sensors. The position of the target's front edge was marked on the range railing with a permanent marker (see fig. 8). This is referred to as position 1. Next, the target was placed at the five nominal ranges on the railing from position 1. At each target location, the position of the target's mounting foot was marked on the railing with a permanent marker, and radar sensors collected data for a minimum of 1 min. After radar data collection was complete, a NIST steel tape was used to measure the distance from position 1 to each of the five target locations. The average measured range from each radar sensor during the close-target placement (position 1) was treated as a sensor offset. Each sensor's offset was subtracted from its raw data record. Then, an average range value was calculated for each 1 min of data collected during each target placement. The resulting average radar ranges were compared to the steel tape measurements of target placement from position 1. Differences between radar range and steel tape range versus steel tape measured range (distance from position 1) are shown in fig. 9. All radar versus steel tape difference results are within ±1.5 cm.

Figure 9. Results from range accuracy verification test.

2.1.5 Dynamic Liquid Target Test

The final laboratory verification test involved measuring water levels in a small tank to confirm the radar sensor's ability to properly process signals reflected from a water surface, a target similar to that encountered in the field. This test was conducted with the H-3612 in the Chesapeake court yard area using the setup shown in fig. 10: a series of two small tanks and an overhead sensor mount made of wood (constructed earlier during preliminary radar sensor testing). This setup results in the H-3612 radar mounted approximately 2 m above the tank's water surface. During the test, water levels in the tank are slowly raised and lowered using an automated pump system. Even though this test facility is still in development and there is not yet a good reference measurement of water level, results are still useful for a qualitative check to make sure the radar sensor is collecting range measurements to a moving water surface as expected. Results collected with the test H-3612 are shown in fig. 11. During the dynamic liquid target test, the H-3612 sensor performed as expected, capturing range changes resulting from the gradual lowering and raising of the water level in the test tank.

Figure 10. Setup in Chesapeake court yard area used to conduct the liquid target laboratory test.

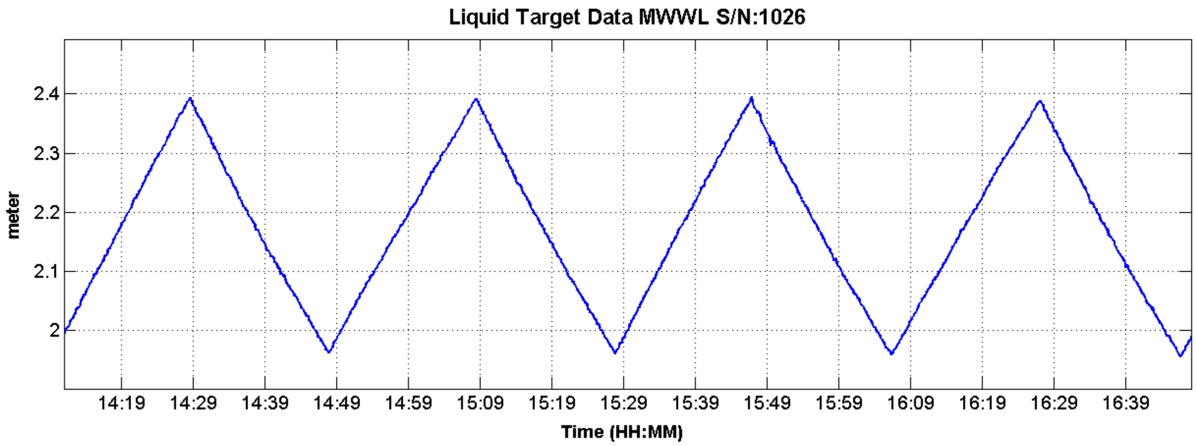

Figure 11. H3612 ranges measured during the liquid target test, while water levels in the test tank were gradually lowered and raised.

2.2. Over-Water Crane Lift Test

An over-water crane lift test recently became part of a standard CIL test procedure that is conducted on all Miros sensors prior to field deployment in operational air gap systems. On 15 August 2011, a crane lift test with a set of three Miros SM-094 air gap sensors (SNs: 020146, 060113, 080427) was conducted by CIL at the Metro Machine facility along the Elizabeth River in Norfolk, VA. Members of the OSTEP team joined CIL to conduct this particular crane lift in order to include an H-3612 sensor (SN 1027) in the test platform.

A full description of the CIL's standard crane lift test procedure is documented in an appendix of [5]. The process involves mounting multiple range sensors in a rectangular-shaped sensor platform that can easily be attached to a crane lift by connecting sections of chain to four eye bolts located on each of the mounting platform's four corners (fig. 12). When hung from the crane, the resulting orientation of sensors in the mount is aiming directly downward. The crane is used to position the sensor platform over a section of water surface. The platform is then positioned over a series of several discrete heights above the water surface and held for a minimum of 10 min at each height. The 10-min time is started after all visually obvious platform motion has stopped. Discrete platform-to-water surface ranges are spaced at 5-m increments covering a range of approximately 5-50 m.

The Metro Machine facility location is narrow and enclosed; therefore, crane lift tests are only conducted on days with low wind so that the section of water surface measured during a crane lift test is typically calm with little surface roughness.

Figure 13 shows a time series of raw 1-Hz range collected from all four sensors during the 15 August 2011 test. The plot provides an indication of the crane-induced range changes that sensors underwent throughout the test.

Although there is no definitive reference measurement of true range on the crane lift test platform, the test setup provides a unique opportunity to assess radar sensor performance in conditions that are close to those experienced in the field. The large area of water surface below the sensor provides an adequate target size for the H-3612 sensor's 8° dispersive beam at long ranges, which cannot be practically accomplished with the horizontal setup with fixed metal target that is described in the laboratory test section 2.1 (in theory, a sensor with an 8° dispersive beam has a footprint that is approximately 7 m when measuring a target 50 m away). Positioning the sensor at a high range over a water surface that is large enough to accommodate the sensor's footprint also provides a good opportunity to record and observe sensor return signals at a series of different ranges.

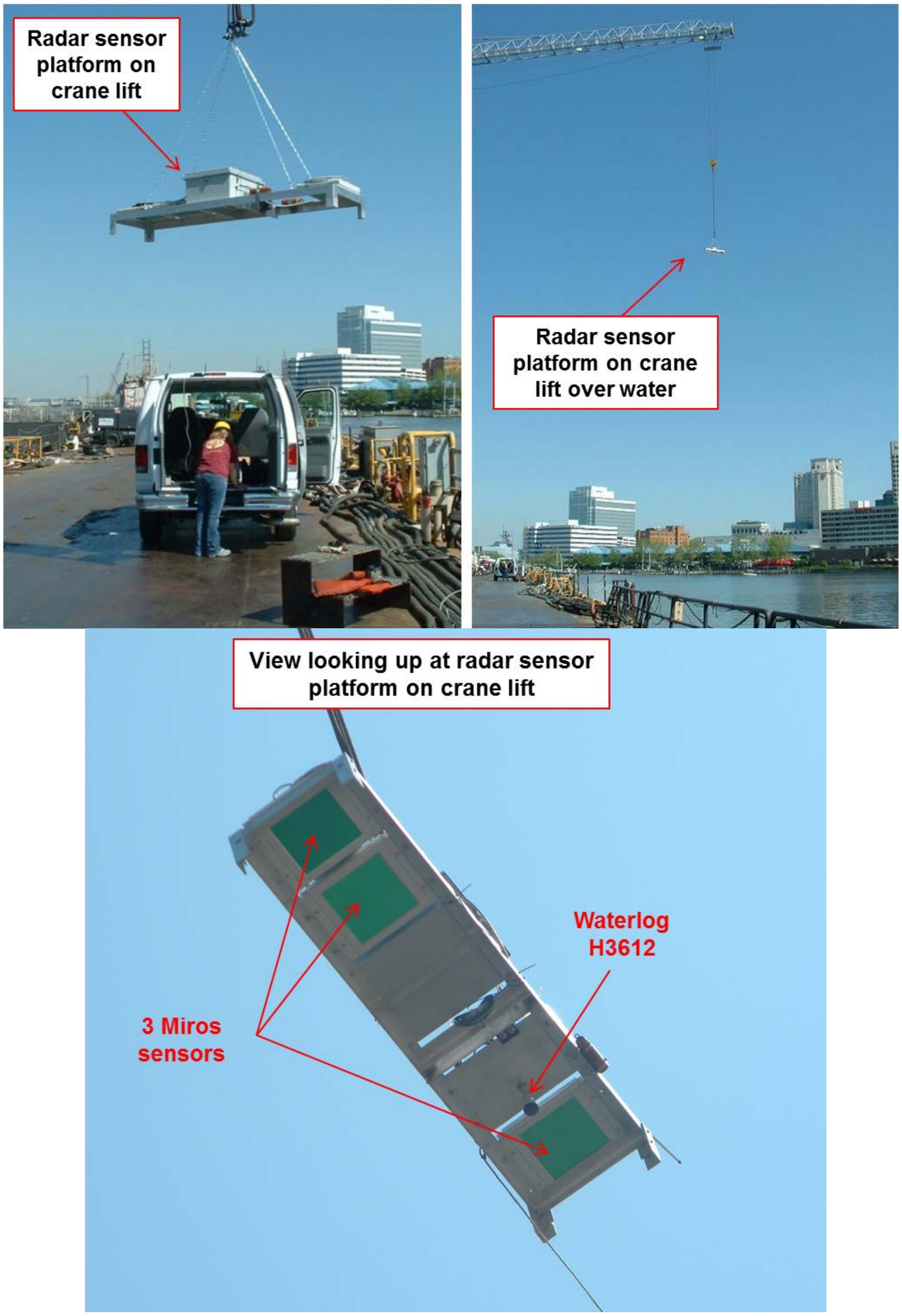

Figure 12. (a) Air gap sensor crane lift test platform at the Metro Machine facility along the Elizabeth River in Norfolk, VA. (b) View from below the crane-lifted sensor platform (looking upward) during the 15 August 2011, test.

Although special care is taken to ensure that the test platform remains level with minimal motion during the 10-min measurement times, there will likely be some platform motion or tilt that will result in a true difference in the sensors' range measurements. Therefore, one recommended method for summarizing data results is to compare each sensor's individual range measurements to an average range taken from the group of all sensors tested. Figure 13 shows one such summary from the data collected during the 15 August 2011 test. First, the average range values of each of the four radar sensors were calculated across each 10-min range stop. Next, a group average range was calculated for each range stop. Figure 14 shows the difference between each individual sensor's 10-min range and the group average range plotted against the group average range. All four sensors showed good agreement, considering potential error due to platform motion and/or tilt; all sensors' range measurements were within ±3 cm. This result indicates that the WaterLog® H-3612 compared very well to three Miros SM-094 sensors.

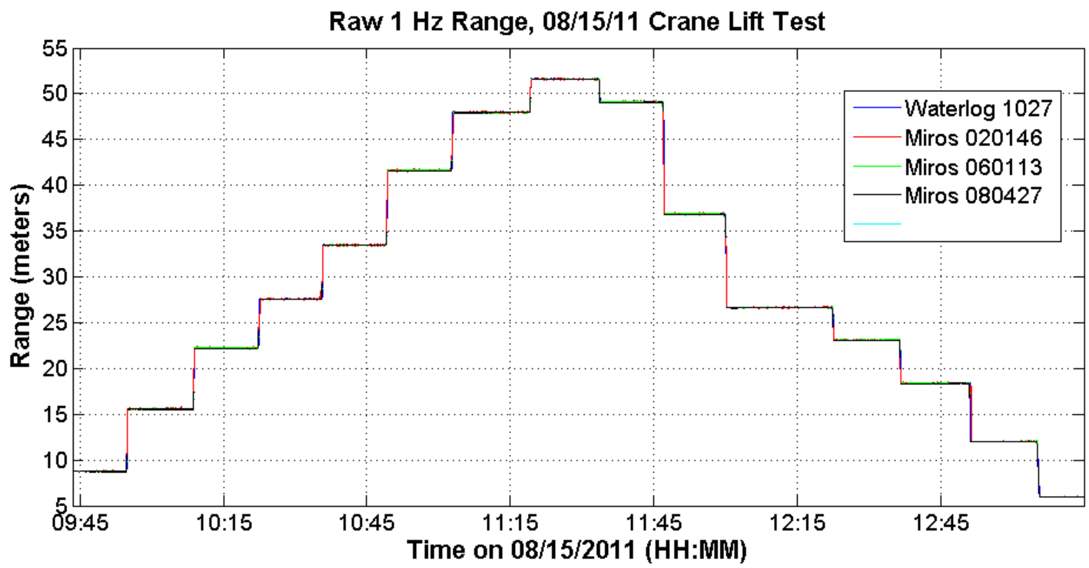

Figure 13. Time series of raw sensor-to-water surface range measured by the four sensors (three Miros and one test WaterLog® H-3612) during the 15 August 2011 over-water crane lift test.

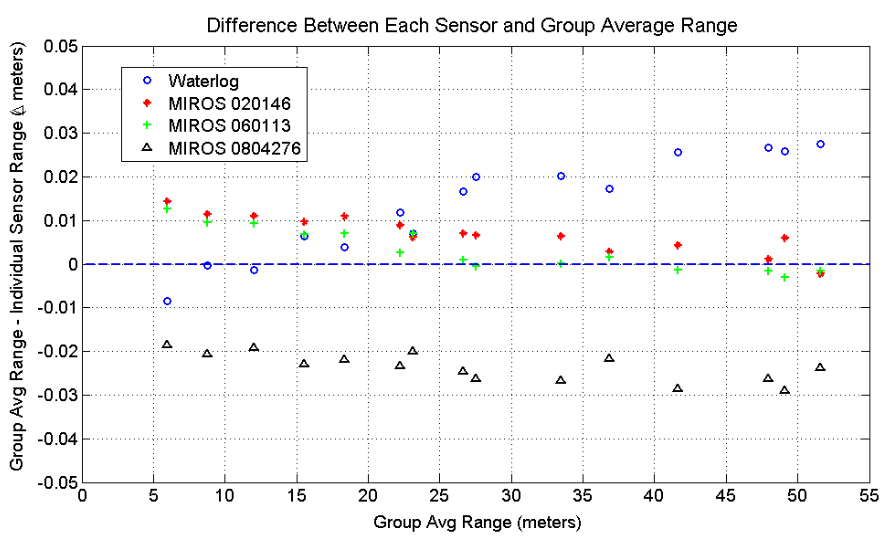

Figure 14. Difference between group average range calculated from all four radar sensors and individual sensors' range readings plotted against the group average range.

During the crane lift test, sample return signals were recorded at each measurement height for the test H-3612. Figure 15 shows two return signal plots generated using the vendor-provided Time of Flight Tool [6] H-3612 interface software: one for the shortest range, 5.62 m, and one for the longest, 53.12 m. Both signal plots show the expected signal characteristics that are required for successful detection and ranging to the water surface, indicating that the sensor was functioning properly. At all measurement ranges during the crane lift test, plots of H-3612 sample return signals showed a distinct peak associated with the water surface, which can be easily selected as the range to the desired target.

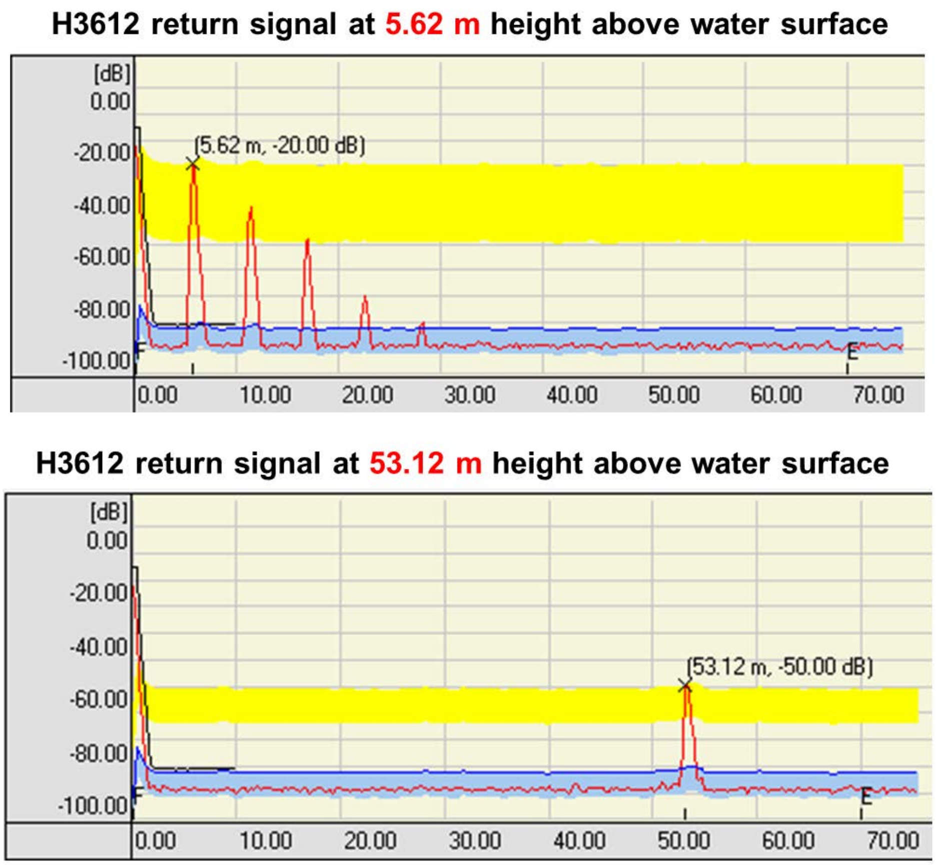

Figure 15. Return signals recorded by the WaterLog® H-3612 at the shortest (5.62 m) and longest (53.12 m) platform heights above the water surface during the crane lift test.

2.3 Field Tests

The final component of the WaterLog® H-3612 radar sensor test involved a field test at the PORTS® air gap station in Reedy Point, DE. On 26 September 2012, a test H-3612 sensor was installed alongside a Miros SM-094 that is part of an operational PORTS® air gap system. The system is located on a bridge across the C&D Canal near Reedy Point. The following section includes a brief description of the test system and the site, as well as a summary of results.

2.3.1 Field Test System

Most of OSTEP's field test systems are assembled with similar base components, which are representative of those of operational systems. The H-3612 air gap field test system employed a Sutron Xpert Data Collection Platform (DCP) along with Satlink for the transmission of data through the Geostationary Operational Environmental Satellite (GOES) system. The latest version of the DCP operating system (v. 3.4.0.6) was accepted by CO-OPS and installed on the Xpert DCP (table 2).

The test system's Sutron DCP and SatLink2 transmitter were installed in an APX weatherproof box, along with three 40-Ah marine-grade batteries, AC-DC battery charger, and a Verizon IP modem. This particular site had 120 VAC power installed in the enclosure, making solar power unnecessary. Other test system components included the WaterLog® H-3612 radar sensor and the GOES antenna. Mounting hardware for the sensor is described in the following section, along with test site details.

The H-3612 was configured to measure and record 6-min range-to-water values in a way that was identical to the operational Miros SM-094 air gap sensor: the CO-OPS DQAP (data quality assurance processing) algorithm was applied to a block of 181 1-Hz samples centered on each 6-min sample time to derive 6-min values. Six-minute range values were recorded to a log, which was stored to the SD card on the DCP. Recorded data were downloaded for post-measurement analysis during site visits and remotely using the IP modem connection. Although the system was configured for real-time data transmission via GOES, GOES-transmitted data were not decoded and ingested into CO-OPS database. Reception of GOES-transmitted data was checked/confirmed on the Chesapeake LRGS (Local Readout Ground Station) to ensure continuous proper operation of the complete real-time system.

Table 2. Test air gap system components.

System Components
Sutron 9210B DCP
Sutron SatLink2 GOES Transmitter
Microcomm GOES Antenna
Raven XT IP Modem
WaterLog® H-3612
PowerSonic 12V 40-Ah Battery (x3)
PowerSonic 12V Battery Charger

2.3.2 Field Test Site at Reedy Point, DE

The bridge at Reedy Point, DE was chosen because of the existence of an operational air gap system for comparison and a collocated OSTEP test platform previously established through an agreement with the U.S. Army Corps of Engineers. The agreement allows OSTEP access to the bridge and some additional space for mounting test systems. The bridge usually has a low volume of traffic, which enhances the safety of on-site CO-OPS personnel.

The Reedy Point Bridge is located on State Highway 9, southeast of Fort Dupont State Park on the Delaware Bay (fig. 16). The site is enclosed and not likely to experience large surface waves, has an average diurnal tidal range of less than 6 ft, and is located near NWLON Station #8551910. The bridge crosses a section toward the east side of Chesapeake and Delaware Canal. The NWLON station is on the south side of the canal, approximately 3000 ft east of the bridge. There is a gravel road to the left of the on-ramp to the bridge from the south, which is a good base camp location for the field crew driver.

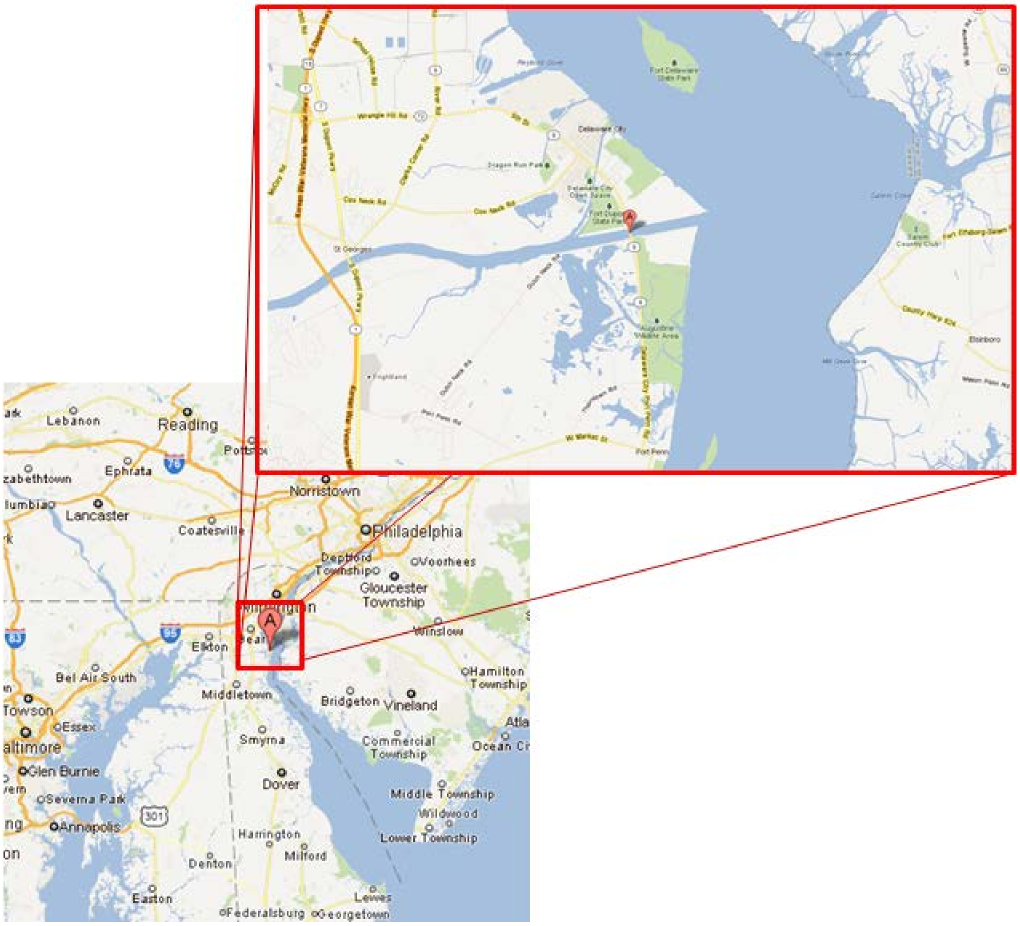

Figure 16. Reedy Point test site; location is on the east side of the C&D Canal.

The sensor platform is located on a cage on the bottom side of the Reedy Point Bridge and is accessed via a ladder that is permanently attached to the side of the bridge. The approximate location is marked by the red arrow in fig. 17. To access the ladder location on the bridge, personnel must put road signs on both entrance points of the bridge, and a driver with safety lights must drop off the field personnel and equipment at a location in the middle of the bridge.

The site is easily spotted by looking for the Stevens brand GOES top-hat antenna that protrudes above the cage, high enough to be seen from the moving vehicle.

Figure 17. Reedy Point Bridge with the approximate location of the air gap system location marked by red arrow.

Test System Installation

The WaterLog® H-3612 test system was installed on the east-facing side of the bridge alongside the operational air gap system with the standard Miros SM-094 sensor. Based on information collected during a reconnaissance trip performed earlier in 2011, a mount was designed by the CO-OPS Engineering Division's CIL and fabricated by Adesso Precision Machine in Norfolk, VA. A conceptual sensor mount design is shown in fig. 18. Detailed engineering drawings are included in appendix A.

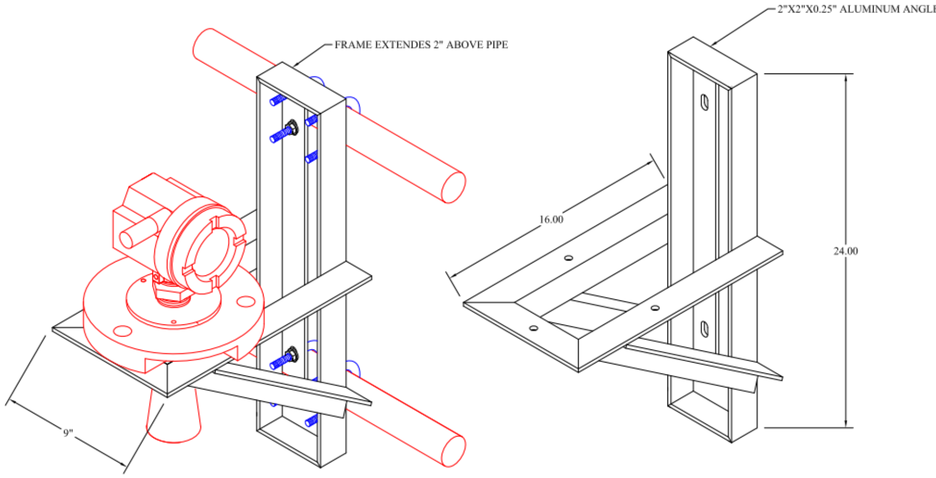

Figure 18. Conceptual drawing (by A. Sanford) of mount used to install the H-3612 test sensor on the bridge.

The H-3612 sensor mount was designed for consistency, stability, and ease of installation to accommodate the standard radar water level sensor leveling collar. The latest version of the collar is lighter and adds the capability to attach Liquidtite fittings to either side to improve resistance to the elements. Detailed engineering drawings for the leveling collar can be found in appendix A.

Figures 19 and 20 show the cage where both the H-3612 test system and the operational PORTS® air gap system are mounted. Figure 20 shows a zoomed-in view of the H-3612 sensor installed in the sensor mount with leveling collar. The mount and collar leveling was performed during installation using a digital level. Leveling was achieved by adjusting three fine-thread screws that attach the plate to the mount to obtain a horizontal angle as close as possible to zero.

The sensor wiring was run through Liquidtite conduit attached to the leveling collar at one end and the APX enclosure at the other end. The hole in the APX enclosure was packed with duct sealant to prevent moisture intrusion.

Never-Seez® lubricant was applied to bolts, since they are made of 316-stainless steel and the mount and collar are made of aluminum. The lubricant will reduce corrosion resulting from contact of dissimilar metals in marine environment.

The series of measured offsets that are applied to vertically align the operational Miros and test WaterLog® sensors' range records in this particular test setup are described in detail in section 2.3.3.

Figure 19. Sensor mounting.

Figure 20. Test H-3612 radar sensor installed on bridge cage railing in mount with leveling collar.

2.3.3 Field Test Data

Data from the test WaterLog® H-3612 system began recording on 26 September 26 2011 and concluded with the tear down and recovery of the test system in early April 2012. Analysis summarized here covers data collected from the test start date through the end of April 2012. The data flow chart in fig. 21 provides a summary of the data coverage for this field test. As shown, a few gaps appear in the first part of the test sensor's record due to an unexpected issue with the test system's DCP. A service visit took place in early November to address the issue, and the successful repair resulted in continuous data throughout the remainder of the testing period. It is important to note that data gaps from the test system DCP failure do not represent a flaw in the performance of the H-3612 sensor. All data from the operational PORTS® Miros sensor at the site are available throughout the entire testing period.

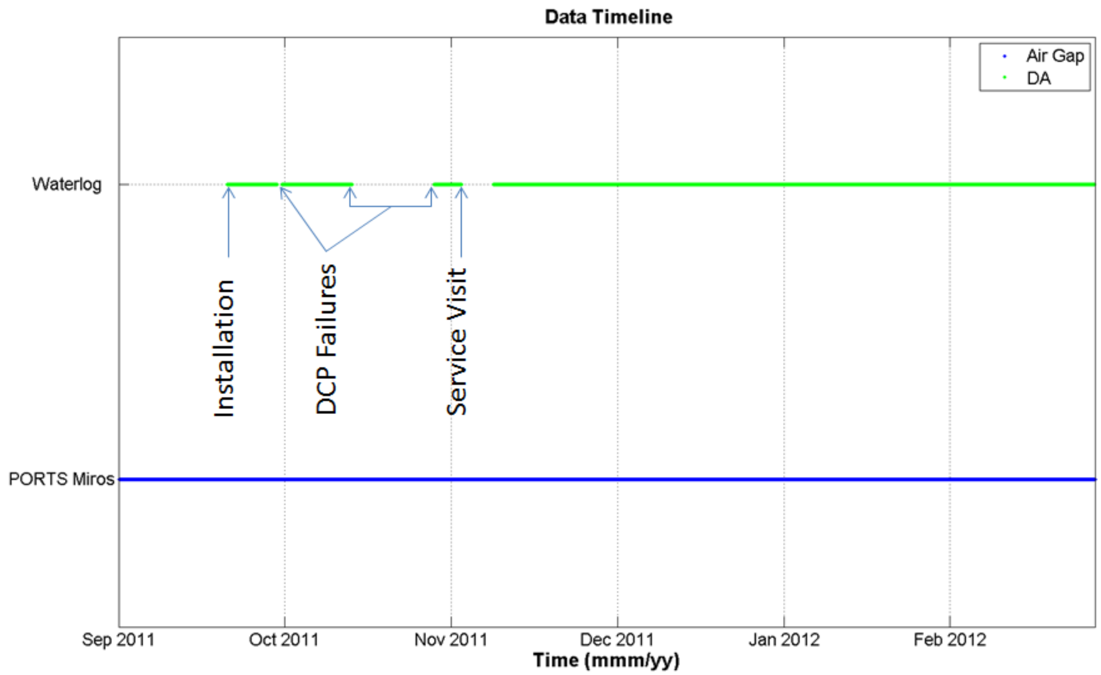

Figure 21. Time coverage of test data

Six-minute average range data recorded by the test WaterLog® H-3612 were remotely downloaded from the DCP using the test system's IP modem; several batches of data were downloaded throughout the test period. Six-minute data from the operational Miros air gap sensor were downloaded from CO-OPS' main data base via the ***DiagTool,*** an internal Web-based tool used for plotting time series data and troubleshooting issues related to data acquisition, data ingestion, and data dissemination. Since these Miros data were the final processed version of the CO-OPS operational PORTS® product, comparative analysis required further processing to derive the Miros sensor's raw range-to-water surface measurements.

Summary of Vertical Offsets Applied to Align Sensor's Range Measurements

A series of vertical offsets are applied to both the test (WaterLog®) and operational (Miros) sensors' data records in order to vertically align the two sensors' range measurements prior to comparison. These vertical offsets are necessary due to the characteristics of both radar sensors, the physical mounting setup of the two side-by-side systems on the bridge, and values that are automatically applied to the operational Miros sensor's raw range-to-water surface measurements during data ingestions and processing. The following paragraphs provide a brief description of the series of vertical offsets applied to both sensors' range records prior to conducting any comparative analysis.

The objective of the offset system described here is to reference both sensors' range measurements to the Miros sensor's zero range point, which is the flat surface of the Miros sensor's planar antenna. To accomplish this, two vertical offsets are applied to the WaterLog® sensor's range record: the sensor offset (SO) and the mounting offset (MO). Two offsets are also applied to the Miros sensor's range record: the in-situ offset (IO) and the lowest steel offset (LSO.) Since data from the Miros sensor used for this analysis are operational data that were downloaded from the CO-OPS main database via the ***DiagTool***, the IO and LSO have been applied automatically upon initial data ingestion. The offsets applied to Miros data prior to analysis presented here involve removing these two offsets from the operational data record to derive raw sensor-to-water surface range. The series of vertical offsets applied to vertically align the two sensors range measurements are depicted in fig. 22 (two WaterLog® offsets in blue and two Miros offsets in red) and listed in table 3.

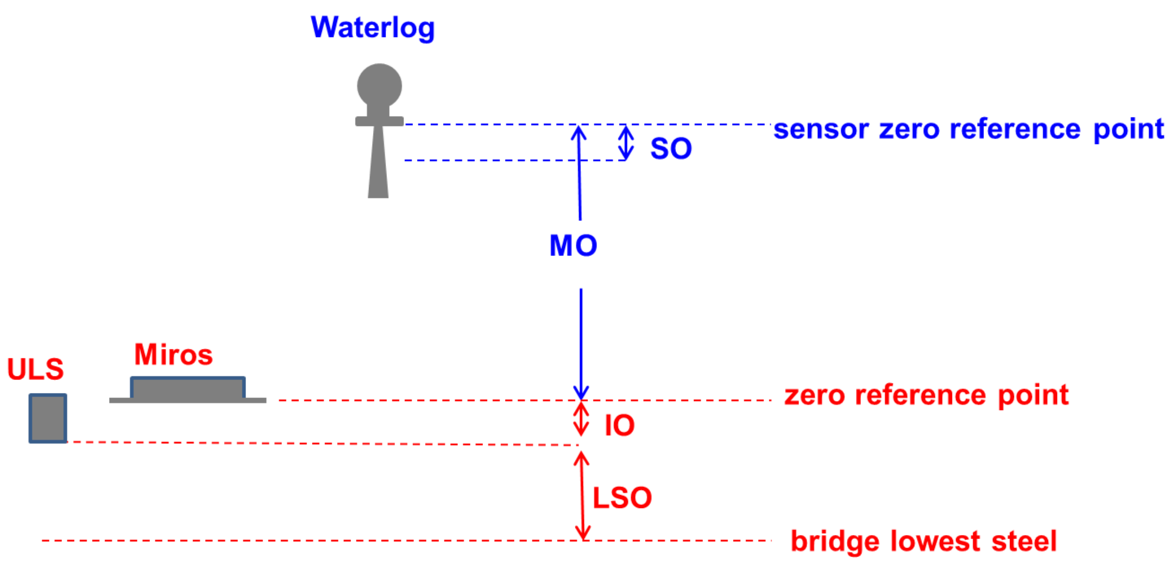

Figure 22. The set of vertical offsets that were applied to each sensor's data records to vertically align range values before comparison.

Table 3. Summary of offsets applied to vertically align sensor's range measurements.

Offset Name	Abbreviation Used in Diagram	Sensor Applied To	Value for Reedy Point Test Setup (m)
Sensor Offset	SO	Waterlog	0.016
Mounting Offset	MO	Waterlog	0.38
In Situ Offset	IO	Miros	1.289
Low Steel Offset	LSO	Miros	0.121

Two vertical offsets are applied to the test WaterLog® H-3612 radar sensor's raw range record. The first is the SO (fig. 23). Although the WaterLog® sensor manufacturer claims that the sensor's zero range point is located on the bottom of the sensor's circular mounting flange for both H-3611 and H-3612 model sensors (fig 23), the sensor's true zero range needs to be measured in the laboratory prior to field installation, as described in section 2.1.2. The difference between the sensor's zero range point and the bottom of the circular mounting flange as measured in the special lab mount is defined as the SO. For the SO example in fig. 23, the sensor's true zero range point is depicted as being below the bottom of the sensor's mounting flange. In this case, the SO will be defined as a positive distance. Sometimes the WaterLog® radar sensor's true zero range point can be above the bottom of the circular mounting flange, in which case it will be defined as a negative distance. Once a WaterLog® sensor is mounted using the radar leveling collar shown previously, the bottom of the sensor's circular mounting flange will be at the same level as the top surface of the leveling collar. As a result, after the sensor offset is applied to the WaterLog® sensor's raw range value (equation provided on following page), the sensor's zero range point can be referenced to the top surface of the radar leveling collar.

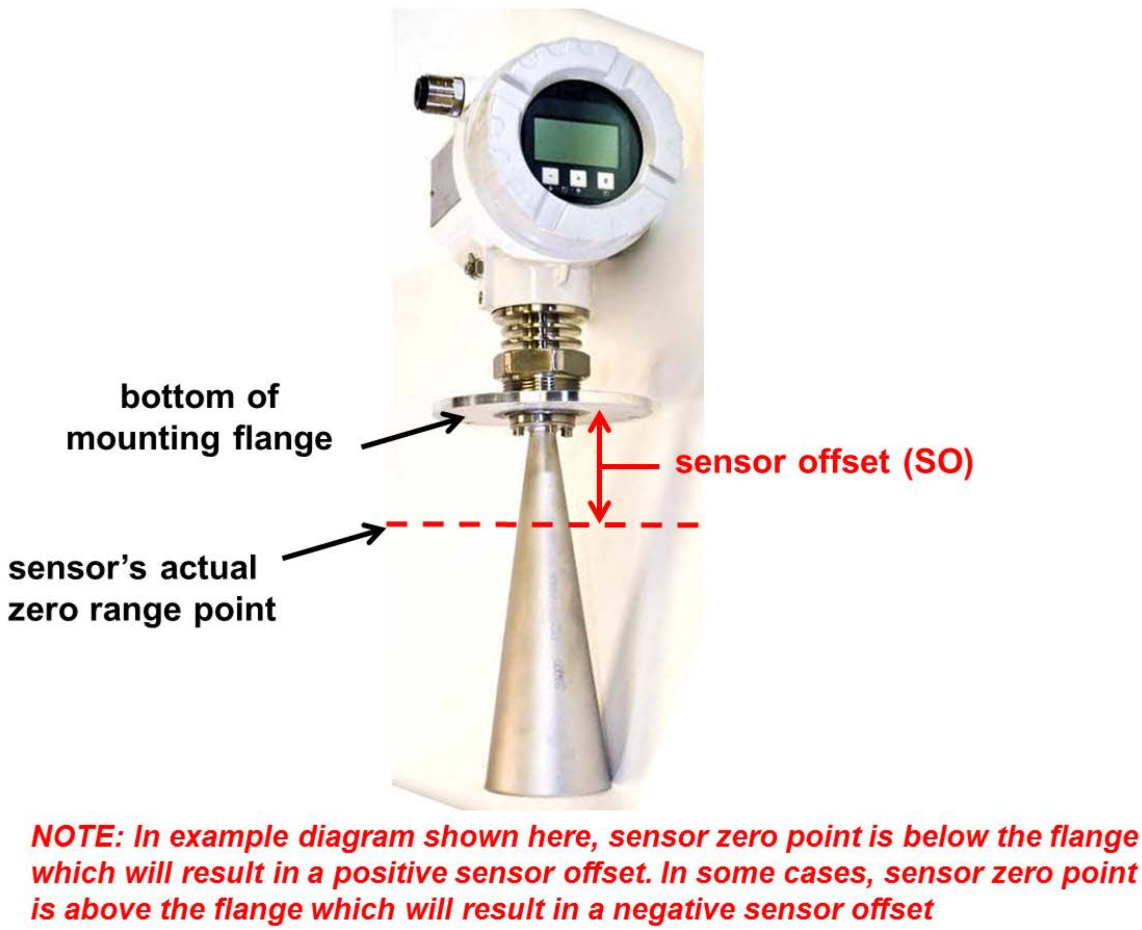

Figure 23. Depiction of WaterLog® H-3612 sensor offset (SO).

The second vertical offset applied to the test WaterLog® sensor is referred to as the MO, which accounts for the vertical separation between the WaterLog® sensor's mounting flange and the Miros sensor's zero range point resulting from the side-by-side mounting setup. Figure 22 shows that the WaterLog® sensor was mounted above the Miros sensor, which was a result of the cage structural design and the space that was available for mounting a new sensor in the platform. The MO was carefully measured multiple times by several observers in the field using a measuring tape in an attempt to quantify measurement precision. The MO measurement point on the WaterLog® sensor was the top surface of the leveling collar (fig. 20) and the MO on the Miros was the flat face of the sensor's planar antenna. A series of four tape measurements were acquired using structural components on the cage's railing as intermediate level reference points. Although special care was taken to measure the most accurate possible MO with a tape and visual reading, (this process was repeated for several trials to confirm high measurement precision), the tape-measured MO will likely be a source of error in final test results presented later in this report. However, since one constant value of MO will be applied to the entire WaterLog® sensor's range series, any MO measurement error will appear as a constant bias across all data. This bias is considered when interpreting final results in section 3.0.

Since the Miros data used in the analysis of this field test were downloaded from the CO-OPS operational database, the two vertical offsets applied for this analysis involve removing two offsets that have been automatically applied during data ingestion to derive a raw sensor-to-water surface range. The first offset is called the IO. The method for derivation and application of this IO was developed by the CO-OPS Oceanographic Division Data Management and Analysis Team during the ongoing development of CO-OPS' existing air gap system. Each operational air gap system includes an LTI ULS installed alongside the Miros sensor, which serves as a supplemental (but not a backup) source of range measurements that are only used for various QA/QC checks. Upon initial installation, the first batch of data collected by the Miros and the nearby ULS is used to derive an average difference between the two sensors' measured ranges. Once derived, this IO value is applied to the Miros sensor's record as a constant to force the sensor's measured range to align with that of the ULS [7]. Although a recommendation for an improved practice is forthcoming, IO is a constant value applied to all operational data collected by the Reedy Point air gap system and needs to be removed to align range measurements to the sensor's zero point.

The second offset that has to be removed from the Miros sensor's operational data record is the LSO, which is the estimated range from the sensor's zero point to the lowest steel on the bridge. The offset is applied to operational measurements to derive a final air gap value that is the distance from this lowest steel to the average water surface.

Equations for applying each sensor's offsets to reference both sensors' range records to the Miros sensor's zero point are as follows. From the WaterLog® sensor's raw range record, R_{wr}, a final range, R_{wf} is calculated as:

$$R_{wf} = R_{wr} + SO - MO$$

From the Miros sensor's operational air gap range record, R_{mo}, a final range, R_{mf} is calculated as:

$$R_{mf} = R_{mo} + IO + LSO$$

All sensor data presented in the following sections start with R_{wf} for the WaterLog® sensor and R_{mf} for the Miros sensor.

Wild Point Editing Data

Spikes, or wild points, caused by vessel traffic passing under the radar sensor's field of view, are common throughout any air gap system's 6-min range record. When a ship passes under a bridge-mounted radar and blocks the sensor's view of the water surface, the sensor detects return signals that are reflected from the ship's structure, resulting in a sudden drop in measured range. In many cases, large ships moving slowly underneath a bridge-mounted radar sensor will affect several subsequent 1-Hz radar sensor range measurements, so the drop in range will appear in 6-min average values even after the DQAP algorithm is applied.

As expected, both data records from the test H-3612 and operational Miros sensor collected throughout the Reedy Point field test contained spikes due to vessel traffic on the C&D Canal. These wild points need to be removed from both sensors' records before comparing sensors' ability to accurately measure range-to-water surface. An automated wild point editing method was designed and applied to both the Miros and WaterLog® sensors' records to remove spikes that are most likely a result of vessel traffic below the bridge. The approach taken involves observing first differences across the radar sensors' 6-min range series and checking against a maximum rate of change threshold.

Data from the Reedy Point NWLON station (3,000 feet eastward on the canal) were used to derive the monthly rate of change thresholds for wild point editing of the two air gap sensors' range records. For each month of 6-min water levels measured at the NWLON station, a series of first differences were obtained by stepping through the entire series and calculating differences between subsequent 6-min values. Monthly histograms of the water level first differences were then plotted to observe 6-min rates of change that are typical for the region; one such example is shown for January 2012 in fig. 24. For each month, the largest 6-min water level rate of change value was used as threshold for wild point editing of the air gap sensors' range records.

By selecting the maximum water level rate of change from the nearby NWLON station as a first difference threshold value for wild point editing the two radar sensor's records, only relatively large wild points will be detected and removed from range records. The method seems appropriate for removing wild points resulting from vessel traffic, since such wild points typically appear as very large spikes in air gap sensors' records.

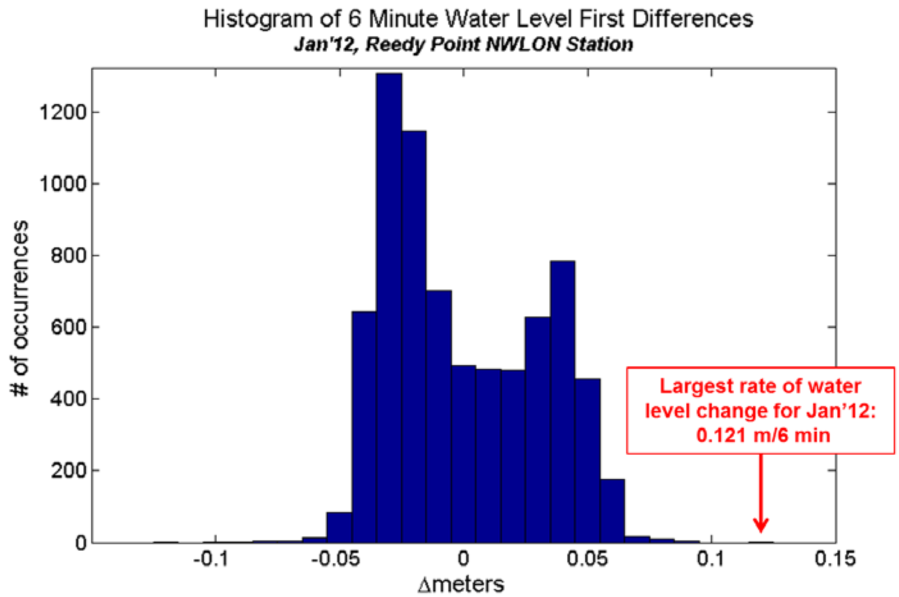

Figure 24. Sample histogram of 6-min water level first difference generated from January 2012 water level record at Point, DE NWLON station.

An automated wild point editing algorithm using NWLON maximum monthly water level rates of change as previously described was implemented in a MATLAB script that is listed in appendix B. This script was applied independently to both the WaterLog® and Miros sensors' records.

Results for each sensor were reviewed to ensure that approximately the same numbers of wild points were detected at approximately the same times in both sensors' records. A summary of wild point edit results is shown in figs. 25-27: Figure 25 shows a sample monthly time series of 6-min WaterLog® H-3612 data collected in January 2012 with detected wild points marked by red circles. Figure 26 shows a summary of wild point occurrences that were detected and removed from both sensors' records, and fig. 27 shows the monthly percentage of data points that were detected as wild and removed from both sensors' records. When viewing fig. 27, note that, due to gaps in the WaterLog® sensor's records (shown in test data coverage plot, fig 20), the total number of monthly data points is smaller than that of the operational Miros for September, October, and November.

Qualitative observations of sensors' monthly time series plots with detected wild points marked, such as the plot in fig. 26, indicate that the wild point method of comparing first differences to a rate of change threshold yield good results; most obvious wild points from both sensors' records are automatically detected and removed. Plots in fig. 27 show that independent wild point edits applied to both sensors' records detect points at approximately the same times for both. Finally, fig. 28 shows that only a small percentage of points were removed from sensors' records and for the five months when sensors' records were equal in length, the total wild points detected and removed were very close for both sensors.

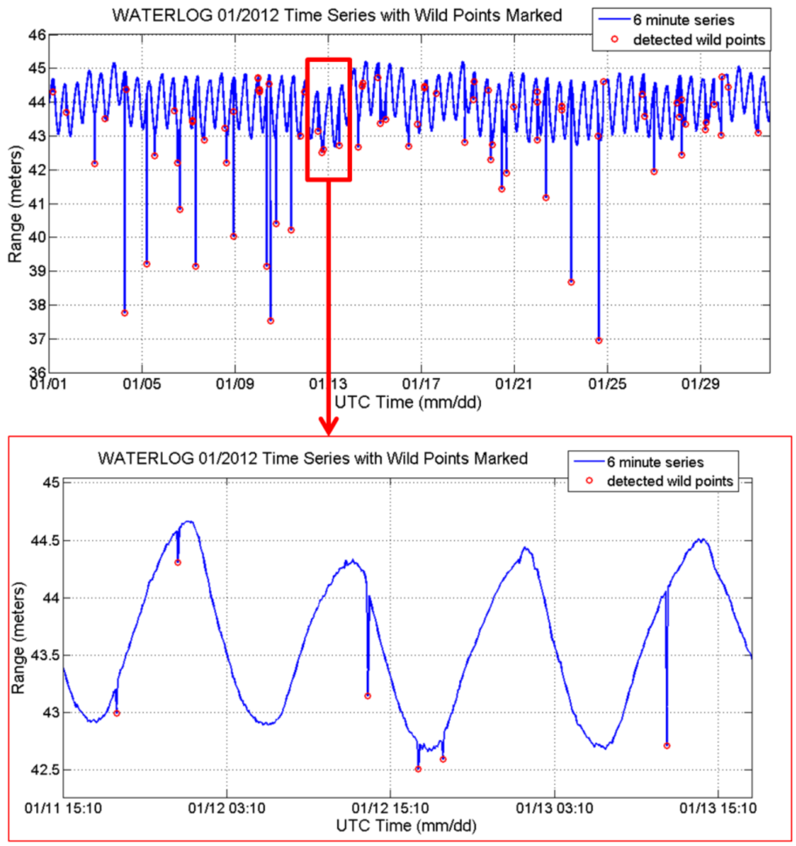

Figure 25. Monthly time series of 6-min H-3612 data collected in January 2012 with detected wild points marked by red circles; bottom panel shows a zoomed-in view of the period from January 11–13.

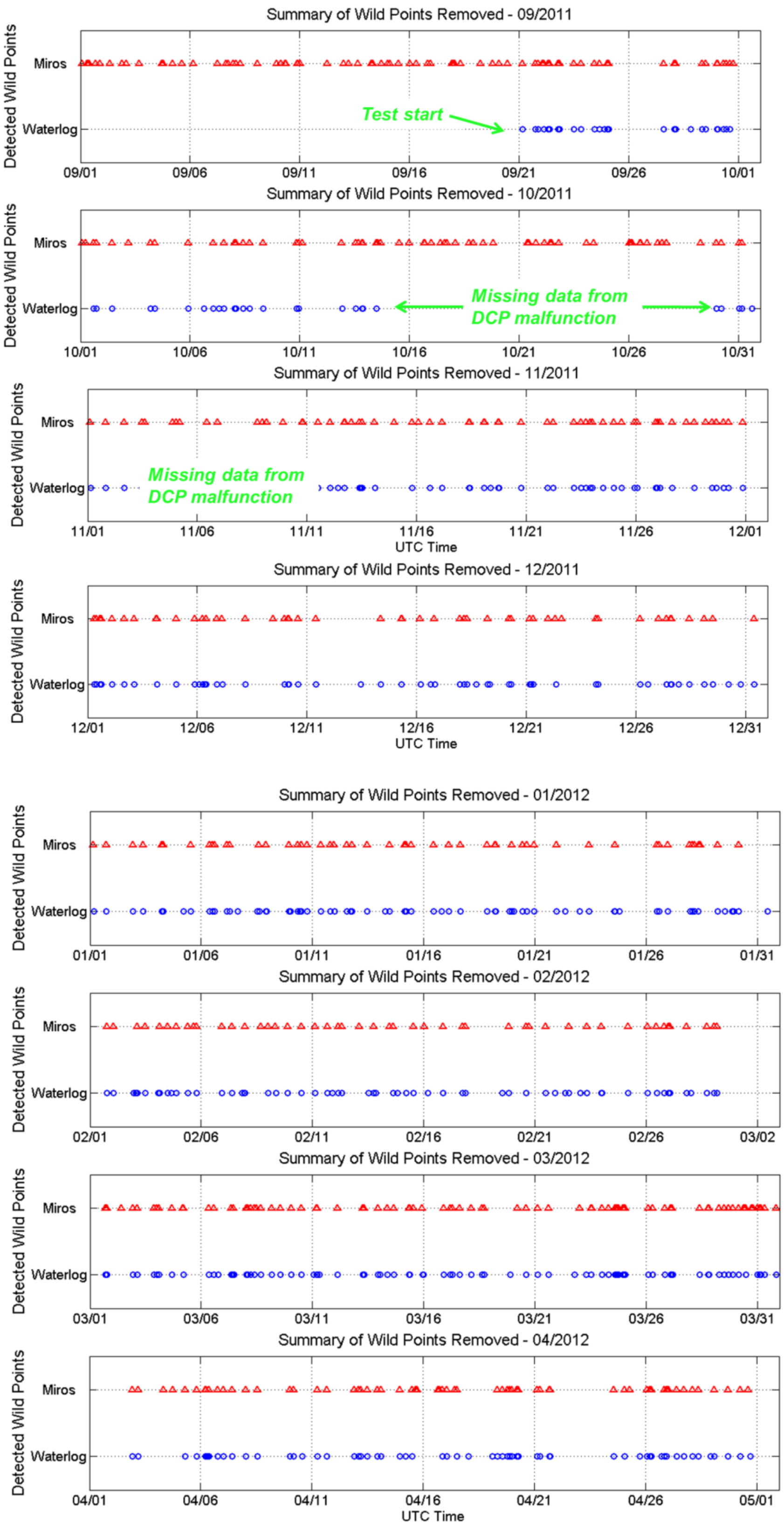

Figure 26. Time and number of wild points detected and removed from both sensors' records.

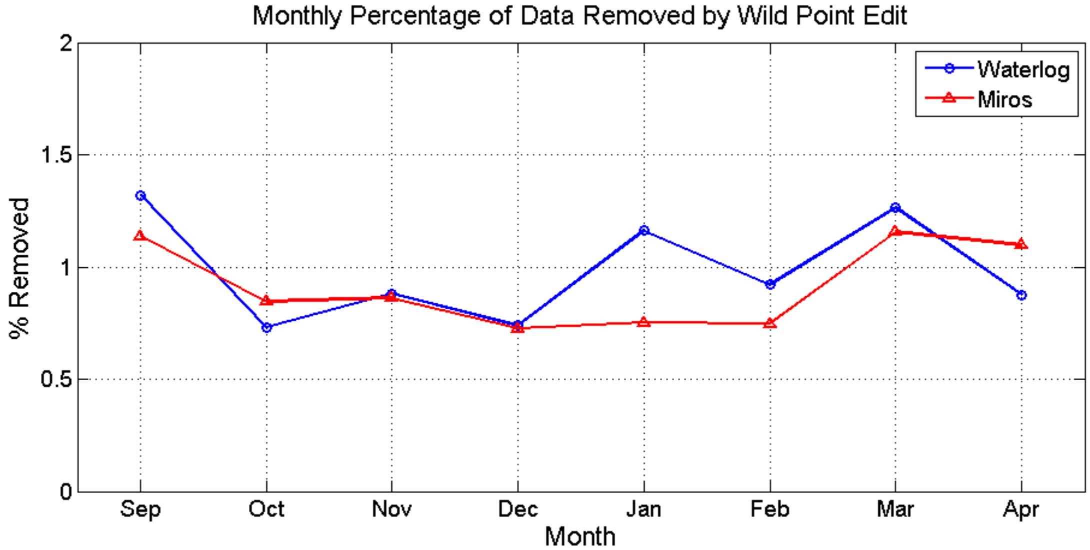

Figure 27. Monthly percentages of wild points removed from both sensors' records.

2.3.4 Field Test Results

All data presented in this section have had wild points removed and vertical offsets applied to align the two sensors' range-to-water surface data, as previously described.

Figures 28 (a)–(h) show eight monthly plots (September through April 2012) of 6-min range-to-water surface measurements from both the test WaterLog® and the operational Miros sensors at Reedy Point (top panel), along with the differences between the two sensors' 6-min records (bottom panel). The difference series were calculated by subtracting the Miros range record from the WaterLog® range record.

Figures 29 (a)-(h) include histograms created from each monthly difference series to show the distribution of sensors' 6-min range value differences. Each monthly difference histogram shows a bimodal distribution. Special care was taken to confirm that the time stamps used by both air gap sensors' measurement systems were precisely synchronized, since subtracting two periodic signals that are slightly out of phase can cause such a bimodal distribution of differences. Both systems were equipped with a Sutron Satlink and GPS antenna that synchronized DCP and GPS times on a regular basis.

Both the difference series in figs. 28 (a)-(h) and the related histograms in figs. 29 (a)-(h) show that on average, the difference in measured ranges between the two sensors is approximately centered on 5 cm throughout the entire record. This 5 cm bias/offset between the two sensors, which remains relatively constant throughout the entire record, may be due to error introduced in the sensor's MO measurement. This measurement was taken using a tape as previously described in section 2.3.3.

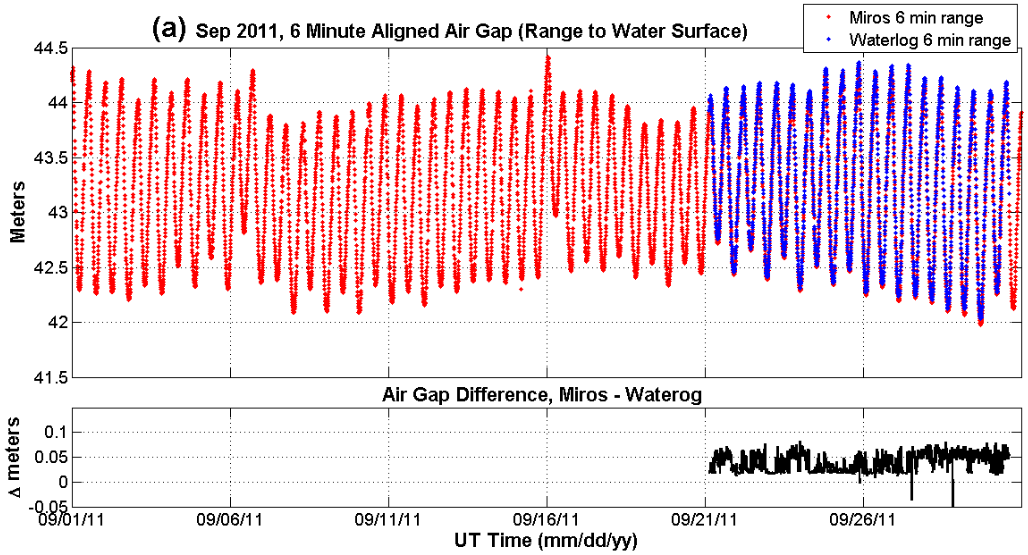
(a) Sep 2011, 6 Minute Aligned Air Gap (Range to Water Surface)
Miros 6 min range
Waterlog 6 min range
Meters
44.5
44
43.5
43
42.5
42
41.5
Air Gap Difference, Miros - Waterog
Δ meters
0.1
0.05
0
-0.05
09/01/11
09/06/11
09/11/11
09/16/11
09/21/11
09/26/11
UT Time (mm/dd/yy)

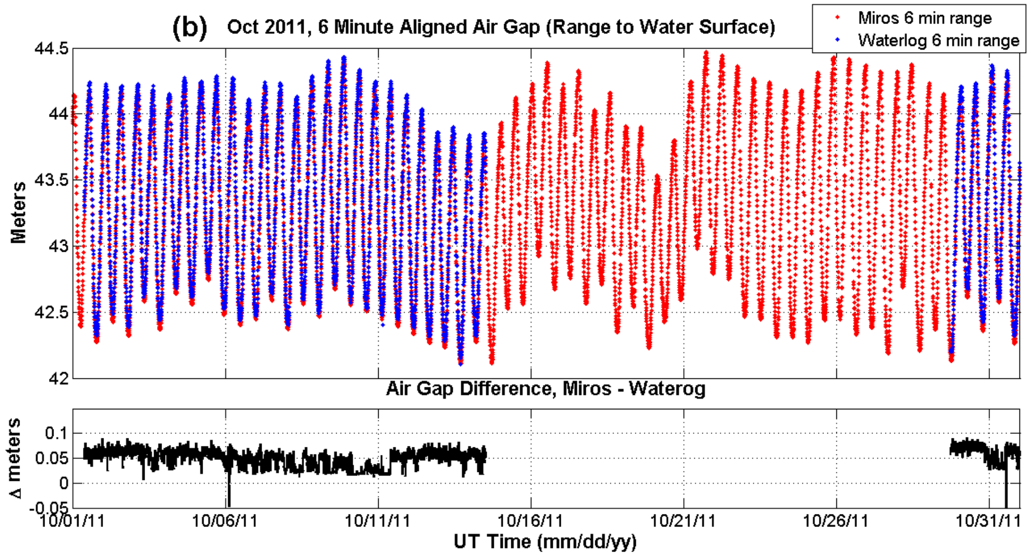
(b) Oct 2011, 6 Minute Aligned Air Gap (Range to Water Surface)
Miros 6 min range
Waterlog 6 min range
Meters
44.5
44
43.5
43
42.5
42
Air Gap Difference, Miros - Waterog
Δ meters
0.1
0.05
0
-0.05
10/01/11
10/06/11
10/11/11
10/16/11
10/21/11
10/26/11
10/31/11
UT Time (mm/dd/yy)

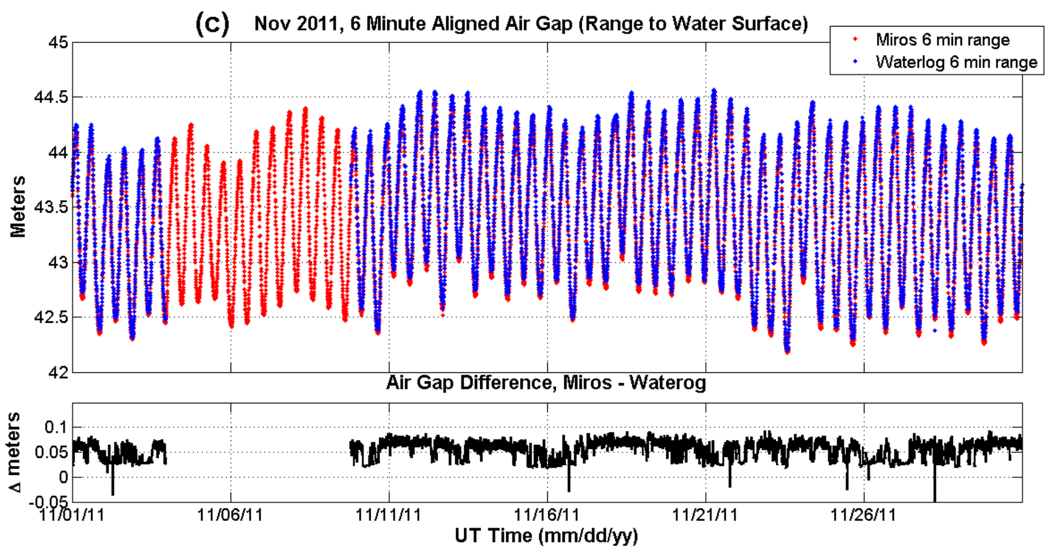
(c) Nov 2011, 6 Minute Aligned Air Gap (Range to Water Surface)
Miros 6 min range
Waterlog 6 min range
Meters
45
44.5
44
43.5
43
42.5
42
Air Gap Difference, Miros - Waterog
Δ meters
0.1
0.05
0
-0.05
11/01/11
11/06/11
11/11/11
11/16/11
11/21/11
11/26/11
UT Time (mm/dd/yy)

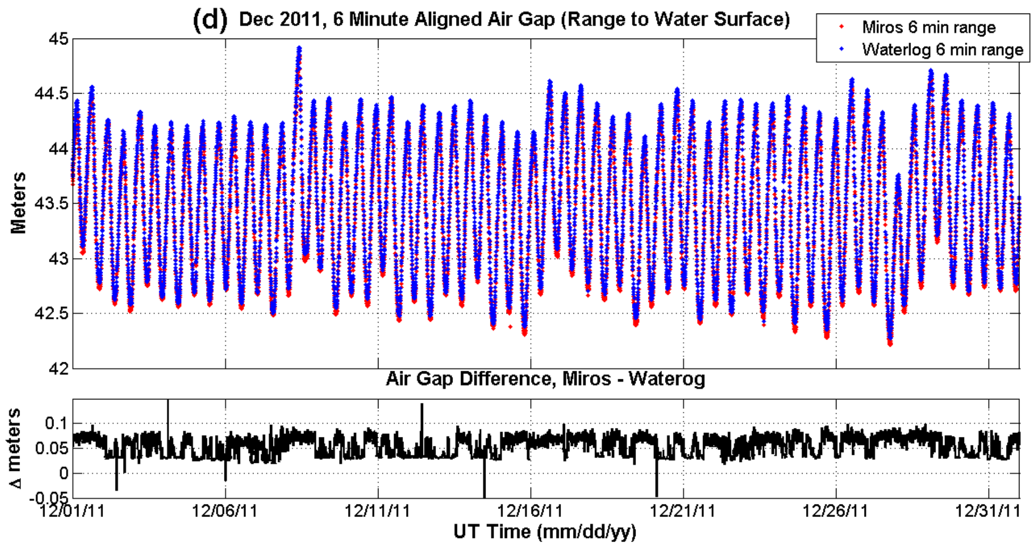
(d) Dec 2011, 6 Minute Aligned Air Gap (Range to Water Surface)
Miros 6 min range
Waterlog 6 min range
Meters
Air Gap Difference, Miros - Waterog
Δ meters
UT Time (mm/dd/yy)

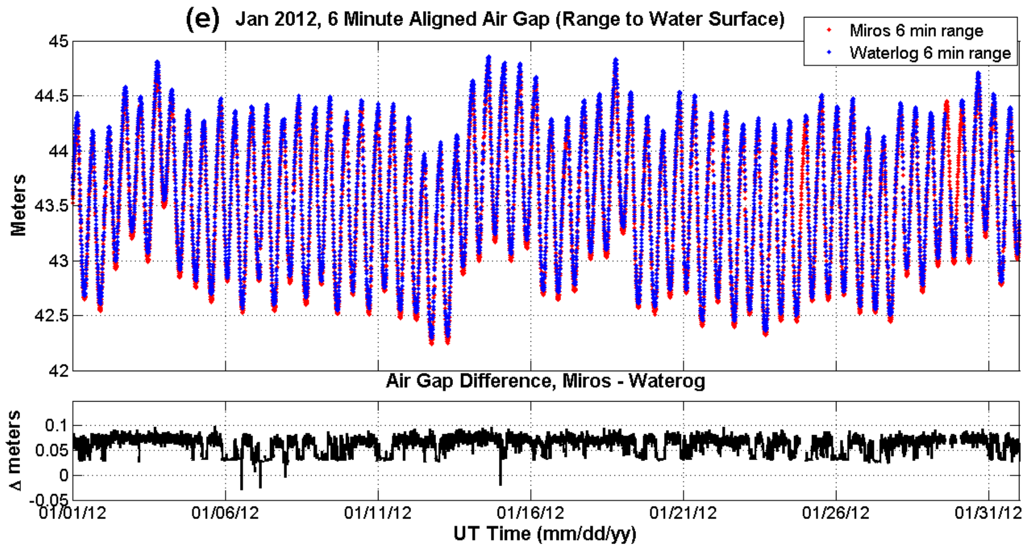
(e) Jan 2012, 6 Minute Aligned Air Gap (Range to Water Surface)
Miros 6 min range
Waterlog 6 min range
Meters
Air Gap Difference, Miros - Waterog
Δ meters
UT Time (mm/dd/yy)

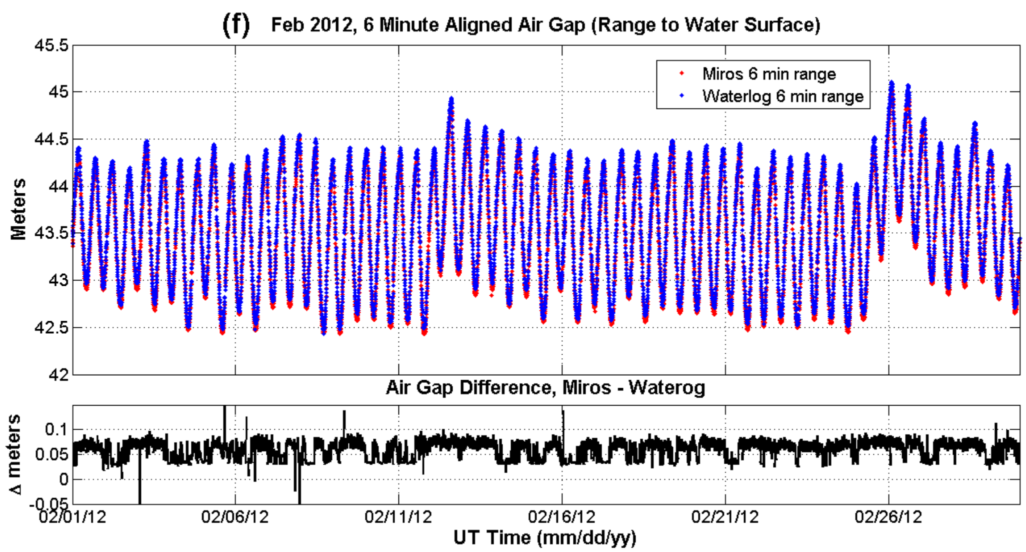
(f) Feb 2012, 6 Minute Aligned Air Gap (Range to Water Surface)
Miros 6 min range
Waterlog 6 min range
Meters
Air Gap Difference, Miros - Waterog
Δ meters
UT Time (mm/dd/yy)

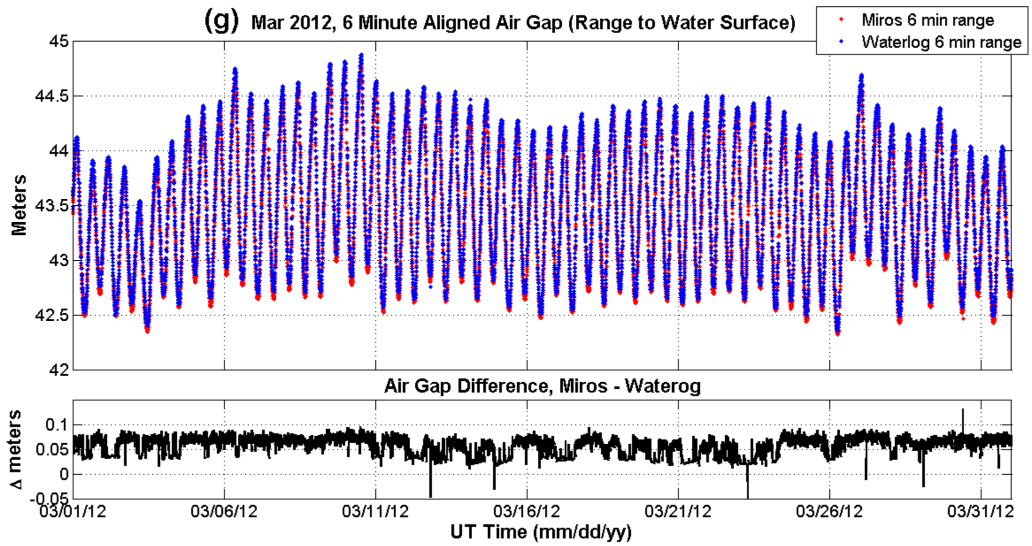

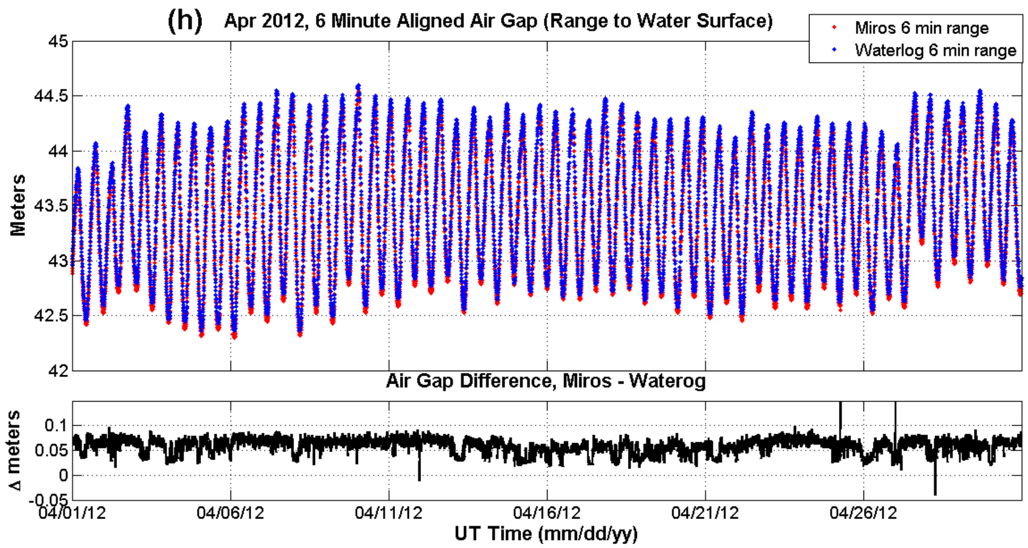

Figure 28. (a)-(h) September through April 2012 monthly time series plots of 6-min range series measured by the test WaterLog® radar and the operational Miros radar sensors (top panel) and the series of differences between the two sensors' measured ranges (bottom panel).

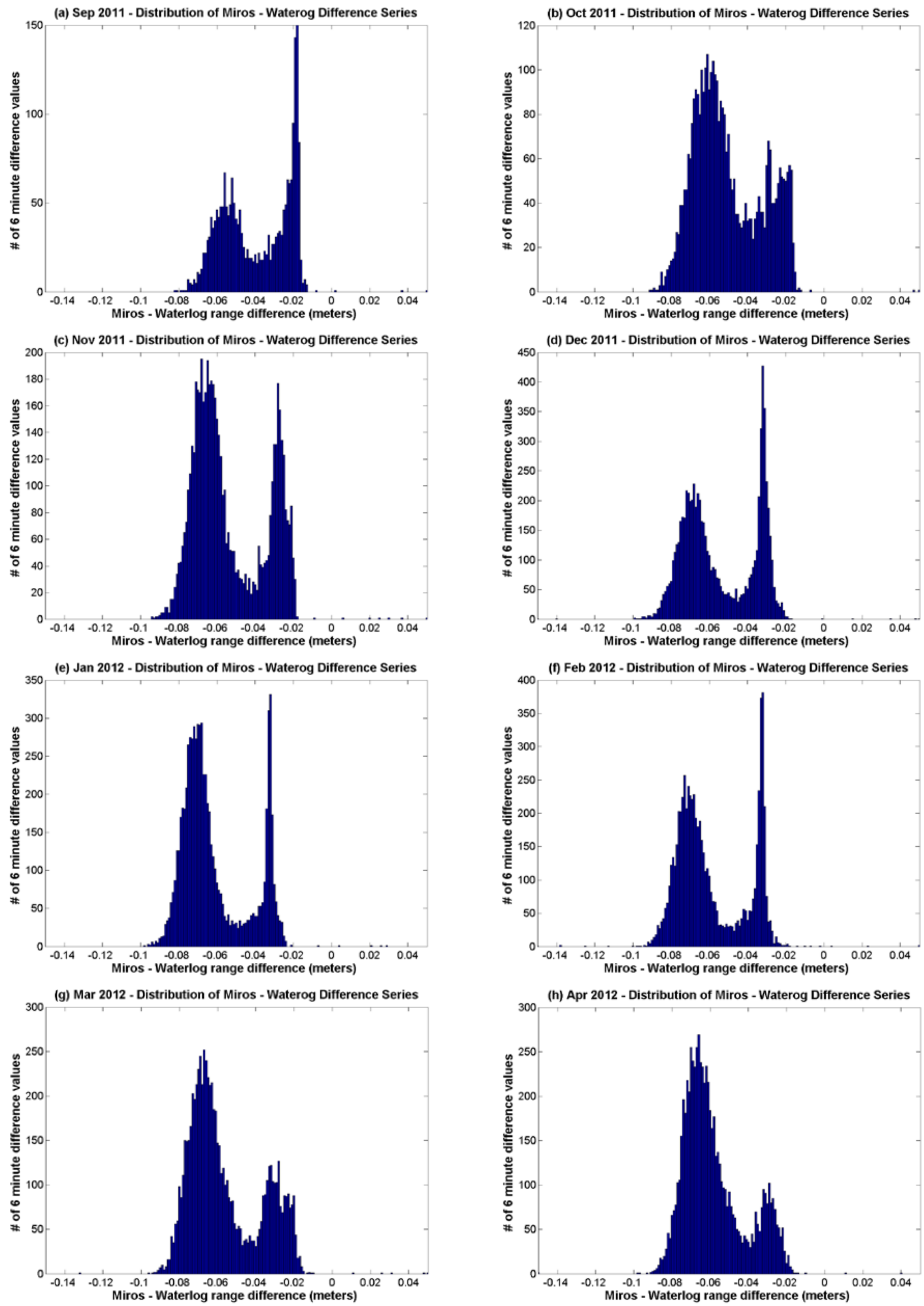

Figure 29. (a)- (h) Histograms created from each monthly difference series to show the distribution of sensors' 6-min range value differences.

Monthly mean differences and monthly root mean squared deviation (RMSD) were calculated from the two sensors' range records shown in figs. 29 (a)-(h). The mean was removed from both sensors' records prior to calculating the RMSD to remove any bias/offset between the two sensors' records that may result from error in the tape-measured sensor mounting offset; the result will provide a comparison of variation only in the sensors' 6- min records. Waterlog® versus Miros monthly mean differences and RMSDs are plotted in fig. 30 and listed in table 4.

When viewing the monthly values, note the gaps that occurred in the test WaterLog® sensor's record due to intermittent DCP failures in September, October, and November (gaps can be seen in figs. 29 a-h). Table 4 includes a column that shows the number of 6-min range values used in the calculation of each monthly value. In addition to data gaps, this sample number also accounts for wild points that were removed from each sensor's record, as described in section 2.3.3. The MATLAB script used to calculate monthly values shown in fig. 30 and table 4 is included in appendix B.

Results show that WaterLog® - Miros monthly mean differences range from 3.9 cm to 6.1 cm, while RMSDs are all less than 4 cm. These values are significantly less than the CO-OPS air gap ±15 cm measurement accuracy requirement defined during the initial development of the original PORTS® air gap system [1].

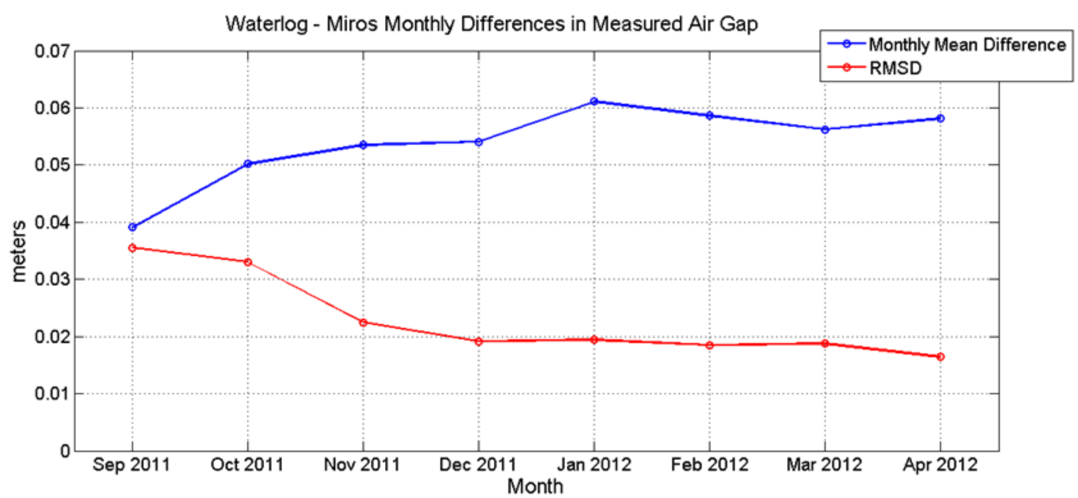

Figure 30. WaterLog® – Miros measured air gap differences; monthly mean differences (blue) and root mean squared deviation calculated after demeaning each sensors' records (red).

Table 4. WaterLog® – Miros monthly mean differences and RMSDs, along with number of 6-min values used for each calculation.

Month	Monthly Mean Difference	RMSD	# of 6 minute range values used in calculations
Sep-2011	0.039	0.036	2241
Oct-2011	0.050	0.033	3668
Nov-2011	0.054	0.022	5727
Dec-2011	0.054	0.019	7371
Jan-2012	0.061	0.019	7222
Feb-2012	0.059	0.019	6839
Mar-2012	0.056	0.019	7329
Apr-2012	0.058	0.016	7092

3.0 Summary and Recommendations

The Design Analysis WaterLog® H-3612 microwave radar offers many advantages for air gap measurement applications. Motivated by the potential to improve existing PORTS® air gap systems, OSTEP conducted a series of laboratory and field tests on the WaterLog® H-3612 to assess the suitability for use in PORTS® air gap applications.

All laboratory tests conducted indicate that the WaterLog® H-3612 meets CO-OPS' operational requirements. Results from field testing at the Reedy Point, DE air gap station indicate that WaterLog® and Miros sensors are in good agreement for 6-min air gap data, with the monthly RMSD less than 4 cm and monthly mean differences less than 6.5 cm; both values are well below the real-time air gap measurement accuracy requirement of ±15 cm, which CO-OPS established with prospective users during initial air gap system development efforts [1]. Based on test results presented here, it is recommended that the Waterlog® H-3612 be accepted for operational use in CO-OPS PORTS® air gap measurement systems where the sensor-to-water surface range will not exceed the sensor's 70-m maximum measurement capability.

4.0 References

[1] Bushnell, M., Bosley, K., Mero, T., 2005. Microwave Air Gap Bridge Clearance Sensor Test, Evaluation, and Implementation Report, NOAA Technical Report NOS CO-OPS O42, Center for Operational Oceanographic Products and Services, National Ocean Service, NOAA, Silver Spring, MD.

[2] Heitsenrether, R. Davis, E. 2011. Test and Evaluation Report - Limited Acceptance of Design Analysis WaterLog H-3611i Microwave Radar Water Level Sensor, NOAA Technical Report NOS CO-OPS 061, Center for Operational Oceanographic Products and Services, National Ocean Service, NOAA, Silver Spring, MD.

[3] Hensley, W., 2011. Pre-deployment Laboratory Test Procedure – Design Analysis Microwave Water Level Sensor Model H-3611/H-3611i. June 22, 2011.

[4] Design Analysis Associates, Inc. 2011. SDI-12 Radar Water Level Sensor Owner's Manual, Version 2.0. Logan, UT. August 22, 2011.

[5] CO-OPS Internal Document, 2011. Field Installation Guide: A Manual for Field Installation and Maintenance Procedures for Deployment of Air Gap Measurement Systems Using the Sutron Xpert 2910B DCP with the Miros Microwave Sensor and the Laser Technology, Inc., Universal Laser Sensor. Version 3.0. November 2011.

[6] Endress+Hauser, 2005. Operating Instructions: Time of Flight (ToF) Tool Operating Program for Intelligent Device #BA224F/00/en/06/05 Version 4.0. June 2005.

[7] Baldelli, S. 2011. Air Gap Database Configuration and Offset Calculation. CO-OPS SOP #3.2.3.5 (E23). Updated June 30, 2011.

List of Appendices

Appendix A.
Engineering Drawings

All drawings in this appendix were created by Albert Sanford (CO-OPS/ED/CIL).

Sensor Mounting Collar

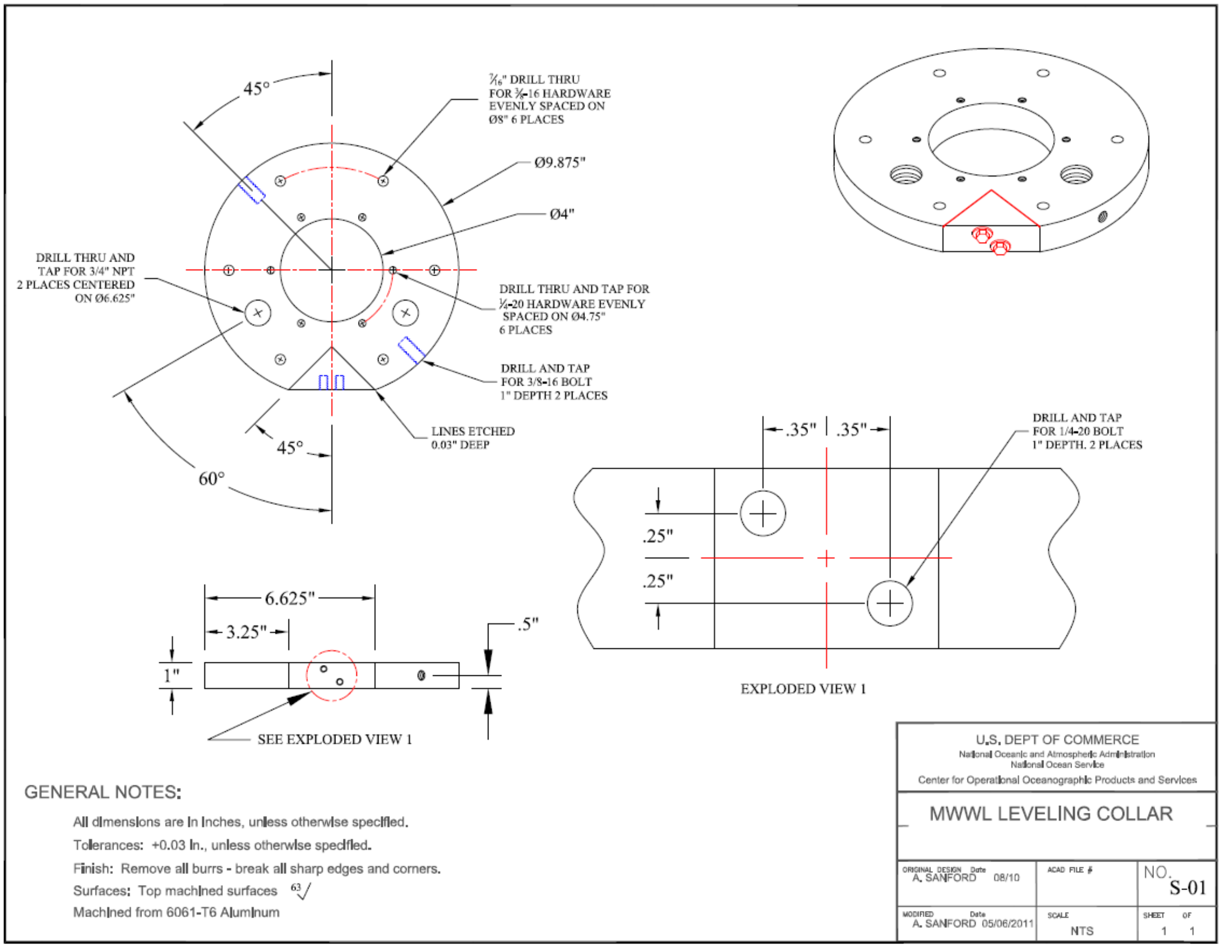

Full Sensor Mount

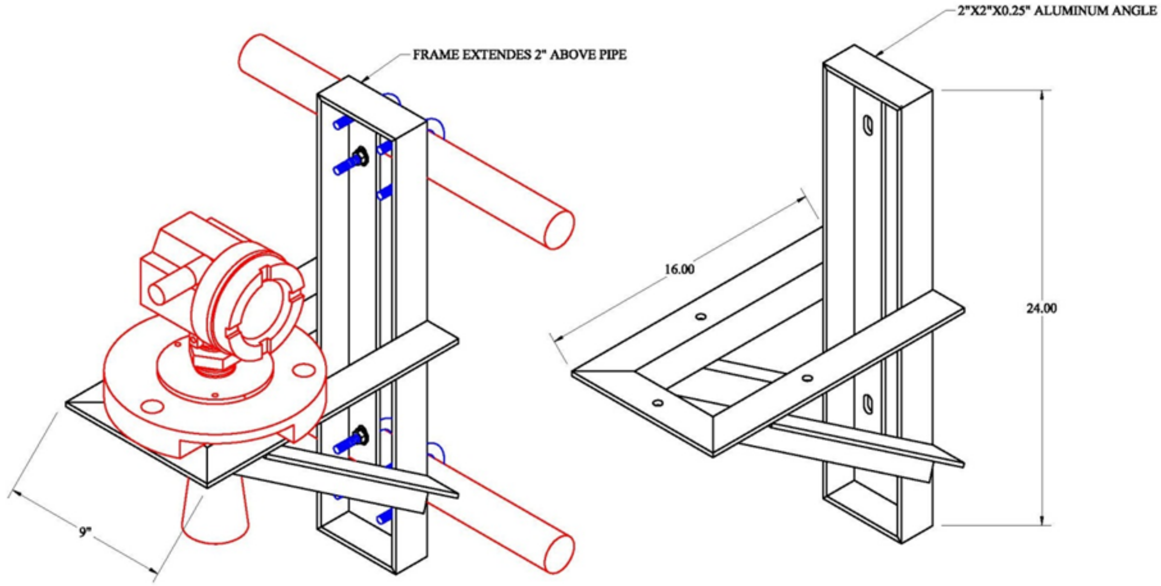

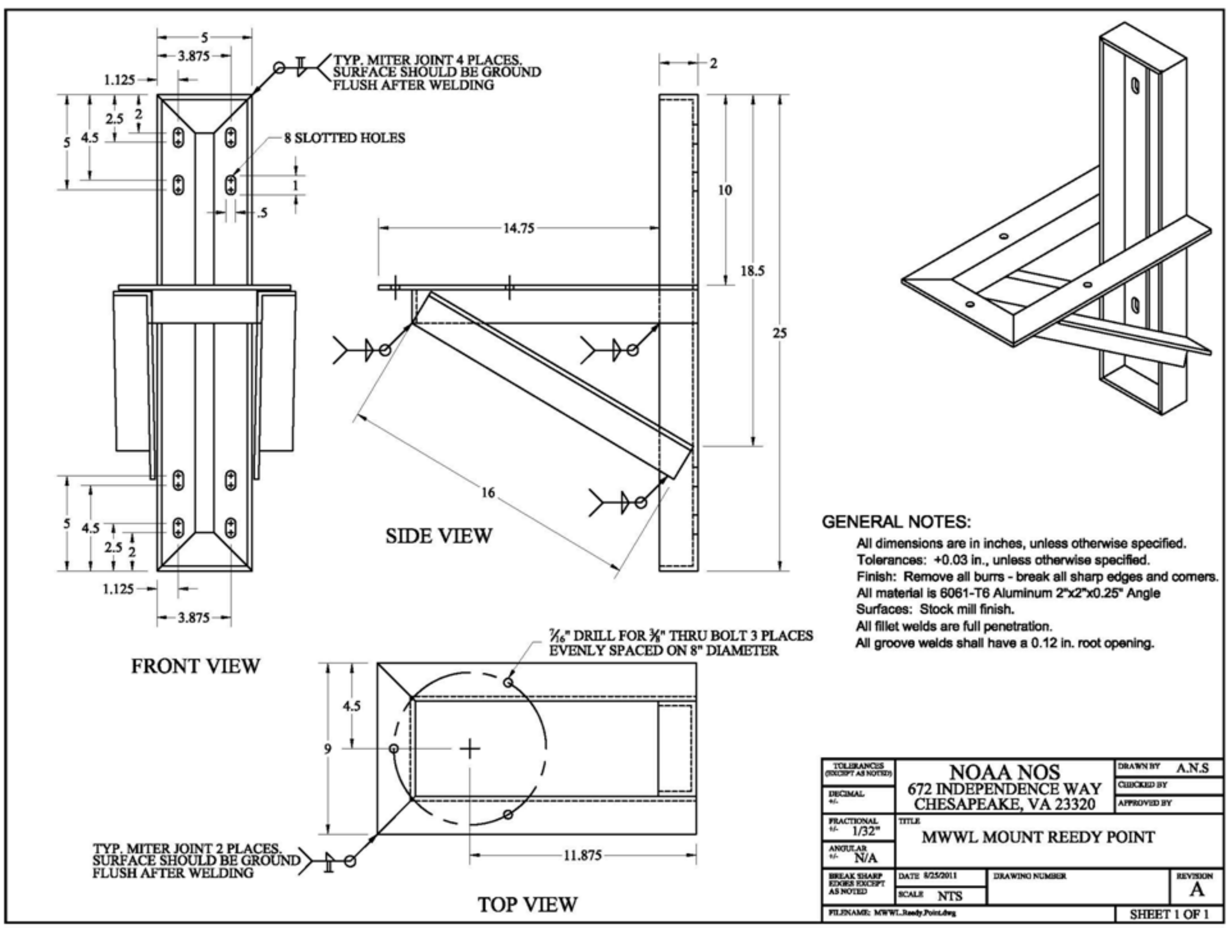

Appendix B. MATLAB Scripts

```
PROGRAME NAME: WildPointEdit_TimeAlignAndSave

% By: Robert Heitsenrether, 05/01/2012

% PURPOSE: Wild point edit air gap data from Reedy Point, DE filed test
% conducted with Waterlog H3612 microwave radar sensor during Sep'11-
% May'12.

% DESCRIPTION: This program performs an automated wild point edit on 6
% minute range measurements collected by both the test Waterlog sensor and
% operational PORTS Miros sensor at Reedy Point. The starting point is 6
% minute range values calculated using CO-OPS DQAP algorithm. Each sensor's
% record is wild point edited independently. The approach taken involves
% loading monthly data files, calculating first differences between
% subsequent 6-minute data points, and checking against a maximum rate of
% change threshold specified for each particular month.


clear all

% directories where 6 minute Waterlog and Miros data reside
loadPath1 = 'C:\Bob\NOAA\AirGap\WaterlogSensors_LongRange\2012_0329_CopyOfFieldDataFromH\FieldTest\Data\mat
files\';
loadPath2 =
'C:\Bob\NOAA\AirGap\WaterlogSensors_LongRange\2012_0329_CopyOfFieldDataFromH\FieldTest\Data\OperationalAG\';

% directories where wild point edited data will be saved
savePath = 'C:\Bob\NOAA\AirGap\WaterlogSensors_LongRange\data_ReedyPoint\data_master\mat\';

% names of data files to be loaded
fileName1 = 'ssp.mat';
fileName2 = '8551911_proc';
dirNames = ['201109'; '201110'; '201111';,...
            '201112'; '201201'; '201202'];

% Monthly water level rate of change thresholds taken from Hensley 03/27/12
% file: PlotAirGapTestVsOp_v3.m. Values correspond to months specified by
% 'dirNames'

  rateOfChangeMax = [0.135, 0.158, 0.204, 0.196, 0.121, 0.138];

%%%%%%%%%%%%%%% WATERLOG AND MIROS - loop through monthly data files and WPE all data
for i1 = 1:size(dirNames, 1)

    %%%%% MIROS START
        load([loadPath2,dirNames(i1,:), '\', fileName2], 'AGdatenum', 'AGmeasurement');

        range_MIROS = AGmeasurement;
        time_MIROS  = AGdatenum;
        clear AGdatenum AGmeasurement

        refRngIdx = 1;  % reference range index
        testRngIdx = 2; % test range index
        WPcount  = 0;   % wild point counter

        while(testRngIdx < length(time_MIROS))
            % range rate of change
            dWL = abs(range_MIROS(refRngIdx) - range_MIROS(testRngIdx));

            % time difference between two subsequent measurements
                dt = abs(time_MIROS(refRngIdx) - time_MIROS(testRngIdx));

            if dt > datenum(0,0,0,0,6*3,0) % check to see if data gap has been crossed
                % if data gap reached, start over on other side. If first point
                % beyond data gap is truly wild, this will bomb
                refRngIdx = testRngIdx;
                testRngIdx = testRngIdx + 1;
            elseif isnan(dWL) % if test value is a NaN, skip over and test next point
               testRngIdx = testRngIdx + 1;

            elseif dWL > rateOfChangeMax(i1) % wild point detected?
                WPcount = WPcount + 1;
```

```
            WPtimes(WPcount) = time_MIROS(testRngIdx);
            WPidx(WPcount) = testRngIdx;
            testRngIdx = testRngIdx + 1;
        else % no wild point move indicies
            refRngIdx = testRngIdx;
            testRngIdx = testRngIdx + 1;
        end

       clear dWL dt

    end % while(testRngIdx < length(DAdate))

    allWPcount_MI(i1) = WPcount;
    allWPtimes_MI{i1} = WPtimes;
    percentBad_MI(i1) = allWPcount_MI(i1)/length(range_MIROS)*100;

    range_MIROS(WPidx) = NaN;

    % clear out temporary variables before loading next monthly file
    clear WPcount WPtimes WPidx

%%%%% MIROS END

%%%%% WATERLOG START
    load([loadPath1,dirNames(i1,:), '\', fileName1], 'DA', 'DAdate');

    range_DA = DA;
    time_DA  = DAdate;

    % align Waterlog time to match that of GOES transmitted Miros.
     time_DA = time_DA - datenum(0,0,0,0,1,30);
     clear DA DAdate

    refRngIdx = 1;  % reference range index
    testRngIdx = 2; % test range index
    WPcount  = 0;   % wild point counter

    while(testRngIdx < length(time_DA))
        % range rate of change
        dWL = abs(range_DA(refRngIdx) - range_DA(testRngIdx));

        % time difference between two subsequent measurements
            dt = abs(time_DA(refRngIdx) - time_DA(testRngIdx));

        if dt > datenum(0,0,0,0,6*3,0) % check to see if data gap has been crossed
            % if data gap reached, start over on other side. If first point
            % beyond data gap is truly wild, this will bomb
            refRngIdx = testRngIdx;
            testRngIdx = testRngIdx + 1;
        elseif isnan(dWL) % if test value is a NaN, skip over and test next point
           testRngIdx = testRngIdx + 1;

        elseif dWL > rateOfChangeMax(i1) % wild point detected?
            WPcount = WPcount + 1;
            WPtimes(WPcount) = time_DA(testRngIdx);
            WPidx(WPcount) = testRngIdx;
            testRngIdx = testRngIdx + 1;
        else % no wild point move indicies
            refRngIdx = testRngIdx;
            testRngIdx = testRngIdx + 1;
        end

       clear dWL dt

    end % while(testRngIdx < length(DAdate))

    allWPcount_DA(i1) = WPcount;
    allWPtimes_DA{i1} = WPtimes;
    percentBad_DA(i1) = allWPcount_DA(i1)/length(range_DA)*100;

     range_DA(WPidx) = NaN;


    %%%%%% Make sure Waterlog (DA) record is same length as Miros
    %%%%%% record. Fill in any gaps with NaNs
```

```
            disp(['For month ', dirNames(i1,:), ', difference in record lengths = ', num2str(length(time_MIROS)
- length(time_DA))]);

            gapFillCount = 0;
            for ti = 1:length(time_MIROS)
                dt = abs(time_DA - time_MIROS(ti));
                tIdx = find(dt < datenum(0,0,0,0,0,1));
                if isempty(tIdx)
                    range_DA_v2(ti) = NaN;
                    gapFillCount = gapFillCount + 1;
                else
                    range_DA_v2(ti) = range_DA(tIdx);
                end % if isempty(tIdx)

                clear tIdx dt

            end % for ti = 1:length(time_MIROS)

             disp(['# of NaNs added to DA range: ',  num2str(gapFillCount)]);

             range_DA = range_DA_v2;
             time_DA = time_MIROS;




    %%%%% WATERLOG END

   % save monthly wild point edited data in new .mat file with '_WPE'
   % appended to filename

       save([savePath, dirNames(i1,:), '_Waterlog_WPE.mat', ], 'range_DA', 'time_DA');
       save([savePath, dirNames(i1,:), '_MIROS_WPE.mat', ], 'range_MIROS', 'time_MIROS');

    % clear out temporary variables before loading next monthly file
            clear  WPcount WPtimes WPidx
            clear range_MIROS time_MIROS range_DA time_DA range_DA_v2


end % for fi = 1:length(dirNames)

% Plot all results

 for i1 = 1:size(dirNames, 1)
     figure
     hold on;

     plot(allWPtimes_DA{i1}, ones(1,allWPcount_DA(i1)), 'b', 'marker', 'o', 'LineStyle', 'none');

     % axis properties
         set(gca, 'Box', 'on', 'FontSize', 14,....
             'YLim', [0.5, 2.5], 'YTick', [1,2], 'YTickLabel', ['Waterlog'; 'Miros   ']);


     % axis labels
         % get date in title using directory name (dirNames)
         title(['Summary of Wild Points Removed - ', dirNames(i1, 5:6), '/', dirNames(i1, 1:4)],...
             'FontSize', 16);
         ylabel('Detected Wild Points','FontSize', 16);
         xlabel('UTC Time');


 end % for i1 = 1:size(dirNames, 1)
```

Acronyms and Abbreviations

Ah	ampere hour
AC	alternating current
CIL	Chesapeake Instrument Laboratory
cm	centimeter
CO-OPS	Center for Operational Oceanographic Products and Services
DC	direct current
DCP	Data Collection Platform
ft	feet
GOES	Geostationary Operational Environmental Satellite System
GUI	graphical user interface
Hz	hertz
IO	in-situ offset
IP	Internet protocol
LRGS	Local Readout Ground Station
LSO	lowest steel offset
LTI	Laser Technology, Incorporated
m	meter
min	minute
mm	millimeter
MO	mount offset
MWWL	microwave water level
NIST	National Institute of Standards and Technology
NOAA	National Oceanic and Atmospheric Administration
NOS	National Ocean Service
NWLON	National Water Level Observation Network
OSTEP	Ocean Systems Test and Evaluation Program
PORTS®	Physical Oceanographic Real-time System
PSD	power spectral density
QA/QC	quality assurance/quality control
RMSD	root mean squared deviation
s	second
SD	secure digital
SN	serial number
SO	sensor offset
ULS	Universal Laser Sensor
V	volt